Mineralium Deposita (2021) 56:1563–1588
https://doi.org/10.1007/s00126-020-01036-x

ARTICLE

# Chemical and physical heterogeneity within native gold: implications for the design of gold particle studies

Robert John Chapman[1] · David Archibald Banks[1] · Michael Thomas Styles[2] · Richard David Walshaw[1] · Sandra Piazolo[1] · Daniel Joseph Morgan[1] · Matthew Russel Grimshaw[3] · Carl Peter Spence-Jones[1] · Thomas James Matthews[4] · Olga Borovinskaya[5]

Received: 29 June 2020 / Accepted: 7 December 2020 / Published online: 1 February 2021


## Abstract

Studies of populations of gold particles are becoming increasingly common; however, interpretation of compositional data may not be straightforward. Natural gold is rarely homogenous. Alloy heterogeneity is present as microfabrics formed either during primary mineralization or by modification of pre-existing alloys by chemical and physical drivers during subsequent residence in either hypogene or surficial environments. In electron-probe-microanalysis (EPMA)-based studies, the combination of Cu, Hg, and Pd values and mineral inclusion suites may be diagnostic for source style of mineralization, but Ag alone is rarely sufficient. Gold characterization studies by laser-ablation-ICP mass spectrometry linked to both quadrupole and Time-of-Flight (ToF-MS) systems show that only Ag, Cu, and Hg form homogenous alloys with Au sufficiently often to act as generic discriminants. Where present, other elements are commonly distributed highly heterogeneously at the micron or submicron scale, either as mineral inclusions or in highly localized, but low concentrations. Drawing upon our own data derived from individual inspection and analyses of approximately 40,000 gold particles from 526 placer and in situ localities worldwide, we show that adequate characterization of gold from a specific locality normally requires study of a minimum of 150 particles via a two-stage approach comprising spatial characterization of compositional heterogeneity, plus crystallographic orientation mapping, that informs subsequent targeted acquisition of quantitative compositional data by EPMA and/or laser-ablation ICP-MS methods. Such data provide the platform to review current understanding of the genesis of gold particle characteristics, elevating future compositional studies from empirical descriptions to process-focused interpretations.

**Keywords** Natural gold · Microchemical characterization · Trace elements · Hydrothermal gold

## Introduction

The compositional variation of natural gold has underpinned studies that investigate genetic relationships between gold from different occurrences. Bulk Ag contents of gold from specific placer mining operations were used by early studies (e.g., Fisher 1945), to investigate the relationship between economic placers and potential lode sources. This approach provided a refinement to the classical approach of prospecting, which relied on interpreting placer gold abundance, to infer the point of influx from a source. The introduction of more sophisticated analytical techniques, such as electron probe microanalysis (EPMA), significantly advanced the study of gold particles by facilitating analysis of many gold particles from a single locality (e.g., Desborough 1971; Antweiler and Campbell 1977), and permitting researchers to identify multiple compositional signatures within gold from

Editorial handling: A. R. Cabral

✉ Robert John Chapman
r.j.chapman@leeds.ac.uk

[1] Ores and Mineralization Group, School of Earth and Environment, The University of Leeds, Leeds, UK

[2] British Geological Survey, Keyworth, Nottinghamshire, UK

[3] SRK Exploration, Cardiff, UK

[4] Department of Earth Science and Engineering, Royal School of Mines, Imperial College London, Prince Consort Road, London SW7 2BP, UK

[5] TOFWERK AG, Uttigenstrasse 22, CH-3600 Thun, Switzerland

a single locality. This approach was used effectively in studies that established broad compositional types in the context of regional geology (e.g., McTaggart and Knight 1993), and in others that considered the relationship between lode gold and its local placer expression (e.g., Knight et al. 1999a).

Identification of mineral inclusion suites present in gold particles from the same locality provided a powerful additional discriminant in studies of placer-lode relationships (e.g., Chapman et al. 2010a, b; Chapman and Mortensen 2016), and in some instances, specific minerals can constrain conditions of mineralization. For example, Leake et al. (1991) proposed a redox control for Au–Pd mineralization in various parts of the UK, through consideration of the stability fields of selenide mineral inclusions and the nature of hydrothermal fluids required for co-transport of Au and Pd. The term "microchemical signature" was introduced by Leake et al. (1992) during a wider consideration of gold-particle signatures, to describe the approach of combining alloy and inclusion data sets. Subsequent studies interpreted mineralogical and compositional characteristics of gold particles in terms of constraints on condition of formation. Chapman and Mortensen (2006) proposed temperature constraints based on inclusion mineral stability fields and Chapman et al. (2010a) interpreted systematic variation in alloy composition to propose a district-scale auriferous hydrothermal systems using the chemical controls on the Ag contents of Au–Ag alloys defined by Gammons and Williams-Jones (1995).

Recently, the number of placer-lode studies has increased substantially (e.g., in Cameroon: Omang et al. 2015; Dongmo et al. 2018; Fuanya et al. 2019; and Pakistan: Alam et al. 2018), reflecting our increased understanding of placer gold compositional features in terms of their source mineralization. In Russia, similar large-scale studies were used to link economically important gold placers to their source (Lalomov et al. 2016; Zaykov et al. 2017; Svetlitskaya et al. 2018; Gas'kov 2018 and Nevolko et al. 2019). The consideration of Au-alloy composition has contributed to paragenetic studies of hypogene mineralization (e.g., Parnell et al. 2000; Palacios et al. 2001; Arif and Baker 2004; Spence-Jones et al. 2018), and to establishing mechanisms by which gold composition is modified in the surficial environment (Hough et al. 2009). In parallel with the proliferation of regional placer-lode studies, various workers have explored different approaches to gold characterization. Studies of Ag-isotope signatures have focused on generic variation according to gold metallogeny (Chugaev and Chernyshev 2012), in addition to isotopic fractionation during the evolving auriferous hydrothermal system (Argapadmi et al. 2018; Brügmann et al. 2019; Voisey et al. 2019). Lead isotopes have been applied to inform regional metallogeny (Standish et al. 2014) and placer-lode relationships (Kamenov et al. 2013). Crystallographic characterization of native gold suggests that some large Australian nuggets are the erosional products of hypogene mineralization (Hough et al. 2009), and that pronounced Ag depletion of placer gold particles in New Zealand is linked to chemical changes associated with mechanical strain induced by fluvial transport (Stewart et al. 2017).

Currently, an increasing number of studies apply laser ablation inductively coupled plasma-mass spectrometry (LA-ICP-MS) to gold analysis, which permits quantitative analyses at levels far below the limit of detection (LOD) afforded by EPMA (e.g., Banks et al. 2018). The development of LA-ICP-MS approaches to gold analysis is considered in a dedicated section of this paper.

Studies of the compositional and physical features of gold have been joined by a rich inventory of work which focus on the biogenic behavior of gold in the surficial environment (e.g., Shuster and Reith 2018 and references therein). Bioremediated processes by which gold is fixed from solution are now relatively well-understood, with consideration to utility in exploration and placer deposits. Although some of this work involves characterizing gold particles using many of the same techniques described in the present study, we have not rigorously pursued the discussion of such work because our own focus lies in the characterization hypogene gold and its detrital placer expression. Nevertheless, we have referenced relevant studies when discussing processes by which gold particles may be modified in surficial sediments.

Compositional studies that seek to characterize populations of gold particles are, however, prone to various pitfalls. Natural gold is compositionally highly variable, sometimes even within the same mineralizing system (e.g., Townley et al. 2003; Chapman et al. 2010a). Consequently, compositional characterization of gold from a specific locality is dependent upon analyzing an adequate number of particles. Gaining sufficient gold particles for study may be challenging, either because of their scarcity, or because of issues with accessing sampling sites (e.g., problems surrounding location or land/mineral rights ownership). Furthermore, heterogeneity within individual particles can result in unrepresentative compositional data, where only a small proportion of the particle volume is analyzed.

This study addresses these issues through consideration of the nature and degree of variability of compositional heterogeneity in gold particles and has developed recommendations for methodological approaches for future studies. The contribution is based on the collective experience of the authors gained over 30 years of research, during which time approximately 40,000 gold particles have been visually inspected and analyzed. This resource comprises both published and unpublished data and has been augmented by a review of published information (~2500 gold particles) generated by other researchers. The resource is unique not only in the breadth of localities and deposit styles contained, but also because every particle in the authors' collections has been visually inspected to identify both mineral inclusions and

fabric features (in addition to the more usual studies of alloy compositions). While the most complete account of its kind, we recognize that future researchers are likely to identify further alloy and mineralogical associations. Consequently, our first aim is to collate the range of features present in gold particles, both to aid interpretation of results of future studies and to provide a foundation for this new knowledge. Secondly, we have linked these generic compositional alloy fabric features to the timing of their formation to discriminate between those formed in the primary stage of mineralization, late stages of mineralization, subsequent residence in the hypogene setting, and surficial environment. Thirdly, the cumulative experiences of many studies coupled with the appreciation of the variation in gold characteristics have permitted us to develop recommendations for both workflow and sample size, such that researchers can generate robust interpretations of appropriately sized sample sets.

Details of the data sources used in the study are provided in Online Resources 1–3. In addition, Online Resource 4 provides example data sets corresponding to the styles of mineralization discussed during this paper. These data sets provide raw microchemical data describing a total 2175 gold particles from 19 localities. Full details of the sample sets are provided in a summary sheet within Online Resource 4.

## Terminology

In the following, we specify terminology used in this contribution and the reasons for their selection.

i. There is general lack of clarity when using the term "nugget," which has been applied to gold particles of widely differing particle sizes (e.g., Hough et al. 2007; Reith et al. 2010). In common parlance, the term "nugget" is synonymous with a relatively large gold mass and we support the definition of Hough et al. (2007) which uses either a size characteristic (> 4 mm longest dimension) or a mass of > 1 g.
ii. A "gold grain" describes a domain defined by a continuous crystal orientation, whereas a "particle" is a single physical entity commonly comprising several gold grains.
iii. Descriptive terms for gold alloy vary between publications, with many quoting the placer industry standard of "fineness":

$$\text{fineness} = \frac{Au*1000}{Au + Ag} \quad (1)$$

where Au and Ag are expressed as wt.%. Fineness values may be of use in correlating historical placer production with new compositional data (e.g., Chapman and Mortensen 2016). However, they are not favored for studies that interpret gold alloy analyses, as they take no account of other minor metals whose concentration may be significant and informative. Even a cursory web search of the definition of "electrum" yields a range of results, originating from various academic disciplines. We prefer the term "gold alloy" because it is unambiguous and encompasses all concentration ranges of all the alloying metals. The term "gold" is employed in the context of the mineral, whereas "Au" is used when referring specifically to the element, e.g., "wt. % Au content of a gold alloy."

iv. The present study includes data sets describing gold collected from a range of physical environments, including placer-gold particles, eluvial gold particles; particles liberated from samples of ore; and, occasionally, gold particles observed in situ in polished ore specimens. The term "hypogene" denotes gold which has not passed into the eluvial or alluvial environment, and which has been liberated from its lithological host by human endeavor. Gold particles recovered from weathered in situ outcrop are termed eluvial, and those recovered from fluvial sediments are referred to as "placer" rather than "alluvial." We also employ the term "detrital" to describe placer gold particles whose origins are hypogene and which have passed into the sedimentary environment through weathering and erosional processes. Various other workers ascribe the origins of some gold particles found in the surficial environment to biogeochemical driven precipitation (e.g., Reith et al. 2018), and thus our use of the term "detrital" specifically excludes such material.
v. Inclusions of other minerals revealed within polished section are an important source of information. In this study, the term "inclusion" refers to opaque ore-mineral species (e.g., sulfides, sulfarsenides, etc.) unless otherwise stated.
vi. We use the term "sample population" to describe gold particles collected from a specific locality. The term "subpopulation" refers to components of a sample population whose compositional characteristics indicate different origins.

## Characterization of gold particles: analytical methods

### Physical characteristics: size and morphology

The size of hypogene gold particles is highly variable, spanning sub-microscopic blebs in sulfides to large masses of several kilograms. Particle morphology is governed by spatial constraints in the immediate environment of precipitation, which is in turn a function of the paragenesis. This study is primarily concerned with gold particles of sufficient size and mass to be collectable from the placer environment, which generally excludes gold particles exsolved from sulfides and

gold formed as micron-scale thick films within minerals (e.g., pyrite).

Morphological characterization of liberated particles is normally achieved through visual inspection of 2D images, either optically or using a scanning electron microscope (SEM), although 3D imaging of tiny particles chemically liberated from their host has also been employed (e.g., Minter 1999). More recently, X-ray tomography has established the size and shape of gold particles, and their 3D mineral associations within ore samples (Sayab et al. 2016). The morphology of hypogene gold particles is modified during fluvial transport where malleable gold is subjected to successive impacts with bedload clasts. The generic morphological evolution from angular to progressively flakier particles has been used to define criteria that infer different transport histories and environments (e.g., Townley et al. 2003, Melchiorre and Henderson 2019). Several studies have sought to quantify shape change either through measurement of particle axes or through derivation of a shape parameter to establish distance to source (e.g., Knight et al. 1999b; Townley et al. 2003). Currently, there is no standard approach to quantify fluvial transport distance from gold-particle morphology, which is testament to the array of factors which influence shape modification (Youngson and Craw 1999).

### Physical properties: crystallographic orientation relationships

An understanding of the evolution of textures in terms of the spatial and statistical crystallographic relationships between and within gold particles is pertinent to the origins of several heterogeneous alloy textures, which are discussed in a later section of this contribution. Crystallographic orientation relationships can be quantified using electron-backscatter diffraction analysis (EBSD, e.g., Prior et al. 1996, 1999). This surface analysis is conducted using a SEM, with data quality highly dependent on the quality of the particle surface. Traditional polishing approaches using abrasives are inappropriate because they disrupt the surface to produce the Beilby layer (Beilby 1921), in which the original structure has been damaged by cold working. Halfpenny et al. (2013) advocated an approach in which chemical etching was followed by a broad ion-beam polish (BIBP), in which a wide beam of high-energy ions removes a thin layer of the sample without any abrasive damage, thereby avoiding mechanical reworking. Focused-ion-beam (FIB) milling has also been employed successfully for the same purpose (Reith et al. 2012, Kerr et al. 2017).

### Chemical properties: major chemical components of gold alloys by EMPA and SEM

Characterization of geological materials using a SEM, or through electron probe microanalysis (EPMA), either in isolation or in tandem, is a well-established and appropriate approach for gold compositional studies. Qualitative characterization of gold alloy microfabrics, revealed in polished section, is undertaken using the backscattered-electron mode (BSE) of the SEM. The grayscale tone indicates Ag content, such that the degree of heterogeneity either within a single particle (Fig. 1A), or between particles (Fig. 1B), may be visually evaluated. Quantitative analysis of alloy composition can be achieved using energy-dispersive X-ray spectroscopy (EDS) on a SEM, although relatively high limits of detection for minor alloying elements normally restrict this technique to establishing the Au and Ag values.

The largest databases of natural gold compositions are obtained from studies that have used wavelength-dispersive X-ray spectroscopy (WDS) on an EPMA. This approach facilitates characterization of the polished surfaces of gold particles in terms of Ag content and in some cases other minor alloying elements, such as Cu, Hg, or Pd. Compositional studies often consider over 100 particles from each locality, such that any subpopulations are more likely to be identified and defined (e.g., Knight et al. 1999a; Chapman et al. 2010a, b). The large numbers of analyses required usually precludes long EPMA analytical times, which in turn increases the limits of detection. This reduces the precision in measuring Cu, Hg, and Pd, and reduces the ability to measure elements at low concentrations, that may be detectable with longer analysis times. Consequently, the majority of data available from EPMA are restricted to the characterization of gold alloys according to Au ± Ag ± Cu ± Hg ± Pd, with detection limits for Hg, Cu and Pd in the region of 100–1000 ppm.

Commonly employed operating conditions for EPMA of Au alloys are 20 kV accelerating voltage, 50 nA beam current, and a combined on- and off-peak count time of 1 min per element. This protocol allows quantification using the higher energy Cu $K\alpha$ [D1] [D1] and Au $L\alpha$ [D2] [D2] lines, ensuring good precision of the major elements. The use of a 5-spectrometer instrument allows a throughput of ~ 60 microanalyses per hour (e.g., Chapman et al. 2000a). Quantification of Ag, Pd, and Hg is achieved using the $L\alpha$, $L\alpha$, and $M\beta$ x-ray lines, respectively. The lower abundance $M\beta$ line is chosen due to spectral interference between the Hg $M\alpha$ and Au $M\beta$ X-rays, a compromise that necessitates accepting a higher Hg detection limit of around 0.3 wt%. In the overwhelming number of cases, Ag is present in natural gold at concentrations that are measurable by EPMA, but characterization of individual particles using single spot analyses is only representative if the particle is homogeneous. Sample populations are characterized by data sets in which each particle is represented by a single analysis, and therefore, a standard approach to characterizing individual heterogeneous particles is required. Leake et al. (1992) advocated characterizing a gold particle according to the earliest alloy, identified from the spatial relationships observed during BSE imaging. An example is provided in Fig. 1A where the order of alloy

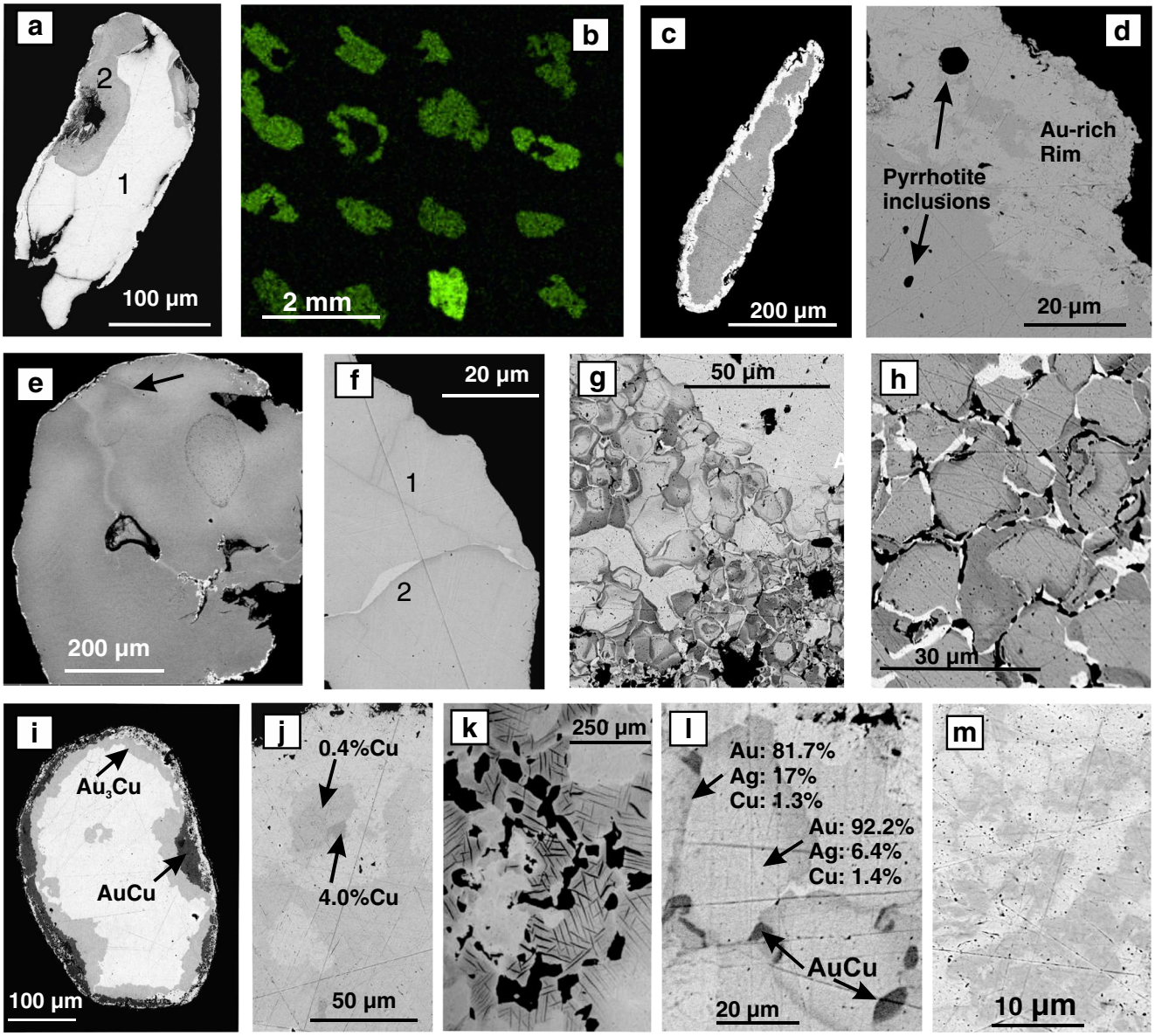


**Fig. 1** Heterogeneity in alloy composition revealed in polished sections and viewed in BSE imaging unless otherwise stated. **a**: Heterogeneous gold particle with numbered points indicating paragenetic sequence of alloy (placer gold particle, Moosehorn Creek, Yukon). **b**: Variation in Au–Ag ratios between placer gold particles indicated by intensity of X-ray map (particles from the Sperrin Mountains, N. Ireland). **c**: Gold particle showing a well-developed gold-rich rim (Bonanza Creek, Yukon, Canada). **d**: Gold-rich rim with inclusion of pyrrhotite within both grain core and rim (Bonanza Creek, Yukon, Canada). **e**: Subtle Au–Ag variation with diffuse boundaries (Boulder Creek, Atlin, BC, Canada). **f**: Thin Ag-rich tracks (1) and a thicker Au-rich /Ag-rich paired track (2) (Wexford, Ireland). **g**: Complex zoned domains confined to one edge of a gold particle (Coffee Creek, Yukon, Canada). **h**: Voids surrounding grains that are partially filled by pure Au (Clear Creek, Yukon, Canada). **i**: Homogeneous Au–Cu intermetallic compounds surrounding a Au–Ag core (River Ayr, Scotland). **j**: Heterogeneity in Cu and Au content, in alloy containing 0.2% Ag (Lake Turkana, Kenya). **k**: Exsolution of AuCu lamellae from patches of Ag-rich (Au: 82.8 wt.%, Ag: 16.2 wt.%, Cu: 1.2 wt.%) alloy adjacent to alloy of Au: 85.8 wt.%, Ag: 13.7 wt.%, Cu: 1–2 wt.%. (Balwoges, Donegal, Ireland). **l**: Compositional modification of Au–Ag–Cu alloy by formation of auricupride during grain recycling (Elatsite, Bulgaria). **m**: Patches of Pd- and Hg-rich alloy (3.2 wt.% Ag, 15.2 wt.% Pd, 22.9 wt.% Hg, dark gray) in matrix (8.9 wt.%Ag, 4.1 wt.% Pd, 6.9 wt% Hg, light gray) (Similkameen River, BC, Canada)

formation is deduced from geometric relationships and is indicated on the figure. The pale gray alloy (labeled "1") is the first phase, and this is partially replaced by darker, high-Ag alloy (labeled "2"). This approach has been adopted in many subsequent studies and provides a standardized methodology for characterizing populations that include both homogeneous and heterogeneous particles (e.g., Knight et al. 1999a; Chapman et al. 2000a).

Inclusions of other minerals are commonly encountered when viewing polished sections of gold particles. These are

primary features, typically 2–25 μm in size, and are inherited by detrital gold particles. Mineral species that are unstable in the surface environment are preserved as inclusions because they are isolated from the atmosphere by their alloy matrix. The presence of inclusions may be established using reflected-light microscopy or, more commonly, by SEM, where dual imaging by BSE and secondary-electron (SE) functions facilitates the recognition of mineral species. In the hands of a skilled operator, the use of reflected-light microscopy removes the need to access an SEM and may generate valuable information. Nevertheless, we prefer the use of a SEM whereby minerals are identified by interpreting EDS spectra, because of the wide range of uncommon minerals which may be encountered and because the potential to identify additional minor elements in certain minerals; e.g. Sb-bearing galena (Chapman et al. 2018). In a few cases, the stoichiometry of individual inclusions has been determined by EPMA so that conditions of precipitation may be more tightly defined (e.g., Chapman et al. 2009).

### Trace-element compositions by mass spectrometry

Quadrupole-ICP-MS systems have been used in several studies to characterize both natural and fabricated gold alloys through quantitative or semi-quantitative measurement of a large range of elements at trace and ultra-trace levels (e.g., Watling et al. 1994; Outridge et al. 1998; Omang et al. 2016; Melchiorre et al. 2017; Banks et al. 2018). More recently, laser-ablation systems have been coupled to time-of-flight (ToF) ICP-MS systems, allowing for simultaneous analysis of all elements in the ablated material. Both approaches have been utilized in the present study.

During LA-ICP-MS analysis, the sample surface is ablated (typically 25 or 50 μm spot size) by multiple laser pulses to form either pits (e.g., Watling et al. 1994), or trenches (Crawford 2007). For quantitative analysis, these ICP-MS systems determine concentrations of trace elements with reference to an internal standard element of known concentration within the particle. Thus, concentrations of major elements must be previously determined for each particle (either by SEM or EPMA) prior to ablation. Quadrupole- and ToF-ICP-MS systems differ in how isotopes are detected in the resulting plasma stream. Quadrupole systems detect each selected isotope sequentially, whereas ToF systems can detect all isotopes simultaneously during a single ablation pulse. Quadrupole systems, which are most appropriate for homogeneous materials, such as gold bullion, were commonly used in early LA-ICP-MS compositional studies (e.g., Watling et al. 1994). However, if the target is heterogeneous (either due to alloy variation or mineral inclusions), it is possible that some component elements will not be recorded during the sequential elemental scan of the mass spectrometer.

Analytical outputs from the quadrupole- ICP-MS systems relate initially to the composition of the surface of polished gold particle and thereafter to the subsurface. In some cases, ablation of subsurface inclusions may be easily inferred, as the elemental signature of the inclusion is clearly visible (Banks et al. 2018). In other cases, it is unknown whether analysis outputs relate to minor components of gold alloy or to full/partial ablation of small inclusions.

Alternatively, ToF systems may be favored as simultaneous measurement can accurately determine any covariance of trace elements. Such an approach allows elemental distribution maps to be generated by rastering 5or 10 μm ablation spots according to a pre-defined grid, to fully characterize the trace-element heterogeneity (see Banks et al. 2018 for a description of the analytical approach using both systems).

Data from LA-ICP-(ToF)-MS will be presented in this contribution as qualitative elemental intensity maps rather than concentrations because this approach facilitates identification of elemental heterogeneity, but avoids the lengthy data processing stage required to convert intensity to concentration values.

### Combinations of analytical approaches

The use of at least two independent data sets greatly aids the identification of subpopulations, which may be particularly useful in the context of detrital-gold studies. Although combining inclusions with alloy compositional data on a particle-by-particle basis is the most commonly used approach to generate a "microchemical signature" (e.g., Leake et al. 1992; Chapman et al. 2000a, b, c; 2010a, b;), synthesis with other data sets, such as gold morphology and alloy composition (Youngson et al. 2002; Crawford 2007; Wrighton 2013; Melchiorre and Henderson 2019; Melchiorre et al. 2017), and crystallographic character and alloy composition (Hough et al. 2009; Stewart et al. 2017), has become more commonplace.

### Graphical depiction of compositional data describing populations of gold particles

**Alloy compositions** Compositional variation between hypogene gold particles liberated from the same ore sample is commonly observed. The core composition of a placer gold particle represents that of the hypogene precursor, and thus compositional ranges of sample populations of placer gold particles represent the range(s) of the contributing populations. Consequently, in most cases, characterization of the population using a single statistical measure of an element or elements is unhelpful. Graphical representations are preferred as (i) they reveal the compositional complexity of gold-particle populations and relative abundance of subpopulations, (ii) they provide an efficient means to compare different

data sets, and (iii) they may integrate other sources of information as extra discriminants.

Gold compositional studies normally involve evaluating the similarity between the concentration profiles of minor elements is different sample populations which contain different numbers of gold particles. Consequently, the most useful approach to graphical depiction permits direct comparison between sample populations irrespective of the number of particles in each. Compositional ranges are commonly depicted using cumulative percentile vs. increasing Ag plots (e.g., Leake et al. 1998; Chapman et al. 2000a). These are produced by arranging all the individual particle analyses within a sample in order of increasing Ag content, against the cumulative percentile of the total number of particles, allowing for direct comparison of sample populations containing different numbers of particles. Plots normally show individual data points, which are more closely spaced in populations with larger numbers of particles. Figure 2A and B shows generic forms of Ag curves, whose shape may be considered in terms of influences on compositional range in the hypogene environment and subsequent mixing of different populations in the placer environment. Curve 1 shows a sample where all particles have the same Ag content, a curve form that is commonly observed in populations of gold derived from small volumes of hypogene ore (e.g., Chapman et al. 2000a, b, 2010a, b). The relationship between the alloy signature of a lode sample and that of the associated placer population is dependent on the degree of spatial variation of alloy composition throughout the eroded material (e.g., Fig. 2A, curve 2). Alternatively, sample populations from placer localities may contain particles from two (or more) subpopulations, resulting in compound signatures. In some instances, compositional ranges may be distinct from one another (e.g., Fig. 2B, curve 1). More commonly, clear breaks in slope indicate two contributing populations, but here it may be difficult to ascribe compositions near the cusp to either of the sub-populations (e.g., Fig. 2B, curve 2).

Compound plots may also result from the analysis of sample populations from a single hypogene source, where they are interpreted to indicate either fluid evolution in a single hydrothermal system (e.g., samples from the Lone Star mine, Klondike; Chapman et al. 2010a), or multiple phases of mineralizing fluid (e.g., hypogene occurrences in the Cariboo Gold District; Chapman and Mortensen 2016). In the context of placer gold, compound plots indicate either a single complex hypogene source, or a mixture of populations from spatially unrelated sources. Thus, sample populations that exhibit either bimodal Ag contents, or a wide range of Ag values, do not necessarily indicate multiple sources. In some cases, establishing inclusion suites can resolve the uncertainty, as subpopulations defined by Ag composition correspond to mutually exclusive inclusion assemblages (Fig. 2C). Online Resource 1 provides an example of analysis of the mixed populations of detrital particles derived from oxidizing chloride hydrothermal systems and orogenic mineralization using several datasets, as do the Russian studies of detrital gold in areas of complex geology (e.g., Lalomov et al. 2016; Nevolko et al. 2019).

**Inclusion assemblages** Inclusion suites can be the best parameter to discriminate between gold generated by different styles of mineralization (e.g., Chapman et al. 2009, 2017, 2018). Various graphical approaches have been employed to depict inclusion assemblages, either based on mineral species (e.g., Leake et al. 1997), mineral classes (e.g., Chapman et al. 2000a), or selected mineral chemistry (e.g., Chapman et al. 2009). Such studies have employed ternary diagrams, either singly or in combination, to apply bespoke discriminants of the inclusion suites and identify mutually exclusive assemblages. Developing a generic methodology for depicting inclusion assemblages has proved problematic, partly owing to the wide range of inclusion species observed, but also due to the amount of data often available. While ternary diagrams

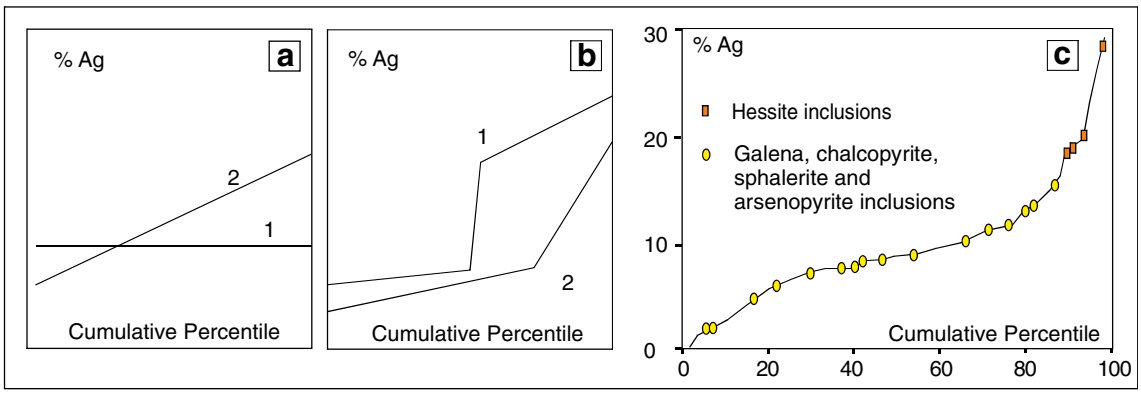


**Fig. 2** Typical shapes encountered in cumulative percentile vs. increasing Ag plots. **a**: plot 1: uniform Ag composition such as that observed in gold particles from the same small volume of ore, plot 2: variation in Ag such as that observed in a placer population derived from a single source. **b**: forms of curve generated by two distinct subpopulations where ranges are mutually exclusive (plot 1) and overlapping (plot 2). **c**: identification of distinct sub-populations using both alloy and inclusion data (adapted from Chapman et al. 2000a, b, c)

continue to be useful, spider diagrams ensure all data are presented, while clearly highlighting important aspects of inclusion mineralogy (Chapman et al. 2017; Moles and Chapman 2019).

## Results

### Physical characteristics of particle surfaces

Rock or mineral fragments inherited from the source mineralization may be present on the surface of gold particles. Quartz is the most common (Fig. 3A), but ore minerals that are unstable in the surficial environment such as sulfides and tellurides may be present in some cases (Fig. 3B). Full or partial coating with Au–Hg amalgam (Fig. 3C) is most likely anthropogenic, a feature of some particles recovered from areas of historical mining. Examination of polished sections by SEM reveals the relationship of surface features, such as partially or fully oxidized ore minerals, to the particle core (Fig. 3D). Embayments filled with either iron oxide or clay sometimes host dispersions of very small (≈ 1 μm) gold particles (Youngson and Craw, 1993). This feature has been observed in gold from hypogene settings (Fig. 3E), and may be inherited by detrital gold particles (Fig. 3F). Thin films of gold may extend into a pyrite matrix (Fig. 3G), and these may survive following pyrite degradation, to yield an array of deformed gold films extending from the particle body (Fig. 3H).

Numerous recent studies of the surface of gold particle have reported small (1–5 μm) "growths" of pure gold (e.g., McCready 2003; Falconer et al. 2006; Craw and Lilly 2016; Shuster et al. 2015; Shuster and Reith 2018). These overgrowths may take the form of crystals or "buds" (Fig. 3I), and their presence appears independent of local climatic conditions (e.g., Reith et al. 2018; Dunn et al. 2019). The relationship between surface authigenic gold and the Au-rich rim is discussed in a later section of this paper.

Crystallographic studies of polished sections by EBSD reveal a number of common features. Figure 4A and B depicts the same particle, firstly viewed in BSE-imaging mode and, secondly, colored according to the grain orientation derived from EBSD analyses. Grain boundaries are invisible in BSE imaging (Fig. 4A, areas 1 and 2), but are identified and fully characterized by EBSD (Fig. 4B). Single colors within a grain indicate consistent orientation (see inset in Fig. 4B), and could

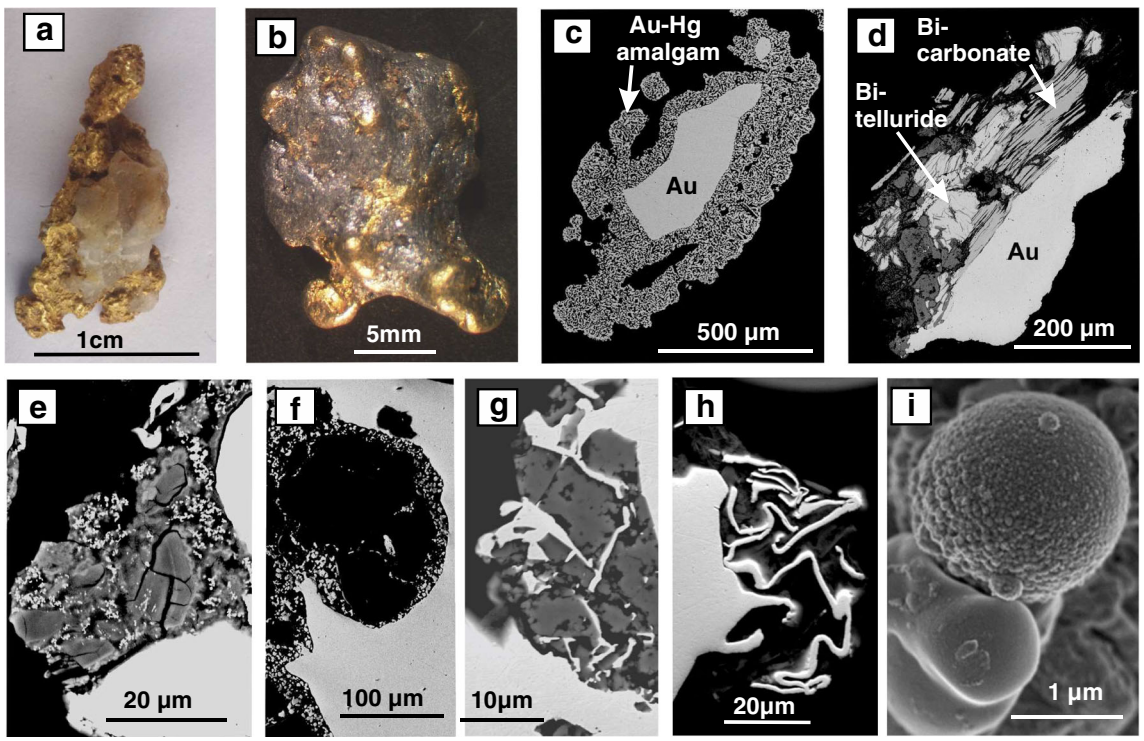


**Fig. 3** Surface characteristics of gold particles (detrital particles unless otherwise stated). **a**: Photograph of a gold nugget that is attached to quartz matrix (Eldorado Creek, Yukon). **b**: Photograph of bismuth telluride mineral (gray) on gold nugget surface (Revenue Creek, Yukon). **c**: Anthropogenic Au–Hg amalgam coating a placer gold particle (Davis Creek, Alaska, US). **d**: Bismuth-telluride altering to bismuth carbonate on the surface of detrital gold particle (Revenue Creek, Yukon, Canada). **e**: Clouds of fine-grained gold (white) in decomposed pyrite (shades of gray) in hypogene particle from Mackinnon Creek, Yukon). **f**: Gold particles that are 1–5 μm across in Fe-oxide matrix, adjacent to a placer particle (Nguiamatsia, Cameroon). **g**: Goethite (after pyrite) infilled by gold (Elatsite, Bulgaria). **h**: Deformed gold films, persisting after the decomposition and removal of pyrite (Sperrin Mountains, N. Ireland). **i**: SE image of surface deposits of pure Au on a placer gold particle from Sardis, Greece

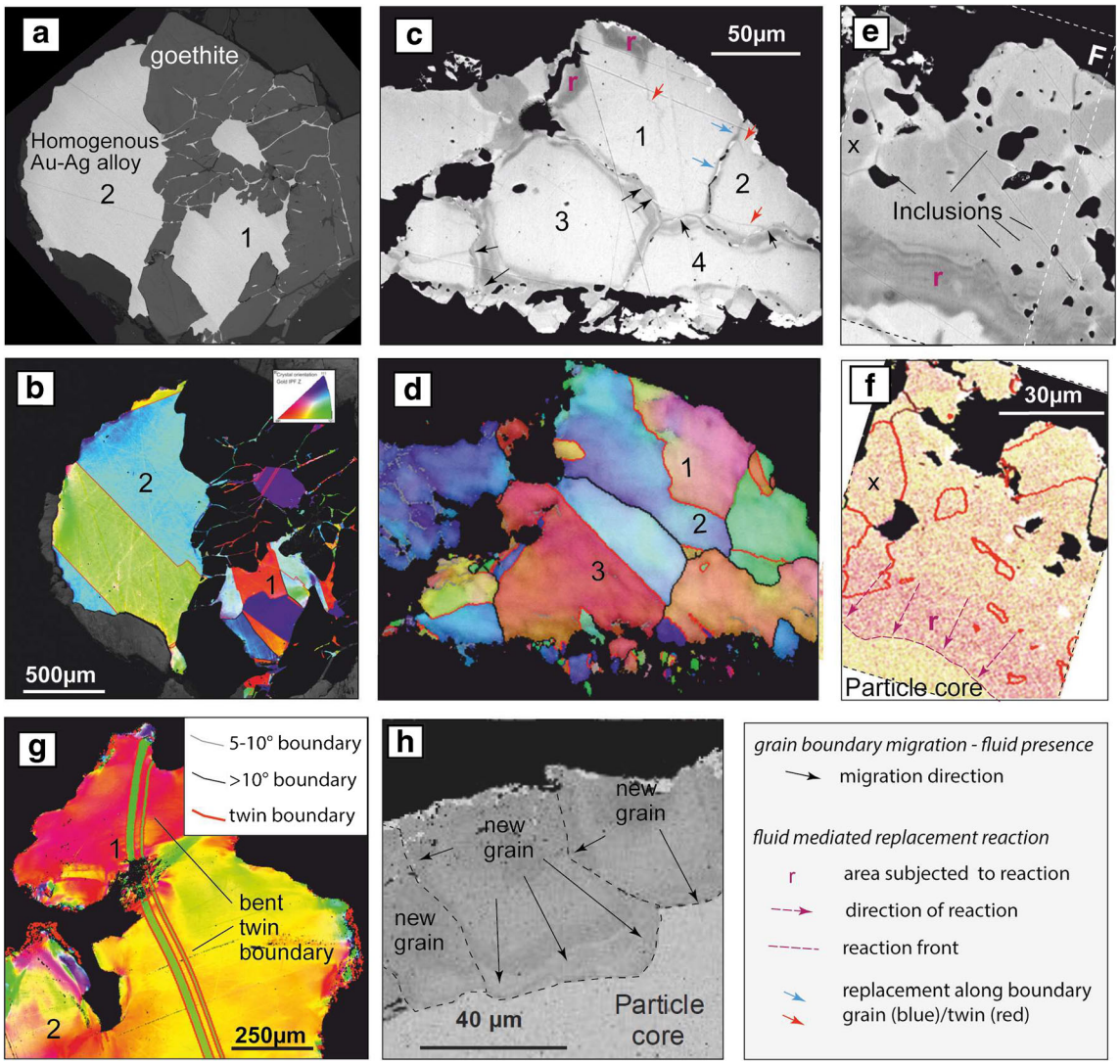


**Fig. 4** Crystallographic orientation relationships of hypogene and detrital gold particles. A, C, D, H: BSE images; darker gray signifies higher Ag amount. (B, C, G) EBSD maps; for color scheme and boundary definition see (B) and (G) inset, respectively. Interpretation of features and their symbols see legend bottom right. **a**: BSE image of a homogeneous gold particle (Au–Ag alloy) from Lone Star, Klondike, Yukon, Canada, intimately associated with goethite (after pyrite). **b**: EBSD map of the same particle as shown in (A); note that individual grains have one color only signifying little internal deformation. **c**: BSE image of placer particle from Borland Glen, Ochil Hills, Scotland, showing distinct areas of different composition; note interpretation signatures. **d**: EBSD analysis of the same particle showing curved twin boundaries (grain 1) and internal deformation of individual grains. **e**: BSE image of another placer particle from Borland Glen, Ochil Hills, Scotland, showing inclusions and changes in composition within a single grain; stippled box shows area shown in (F). **f**: Au-Ag EDS map showing high Ag content as increasing pink coloring; note interpretation signatures. **g**: EBSD map of placer particle from Bonanza Creek, Yukon, Canada; note the internal deformation of grain depicted as color changes as well as the bent twin boundaries. **h**: BSE image of detrital grain from Sperrin Mts, N. Ireland; stippled lines highlight grain boundaries of new grains grown at the edge of the particle. 4A, B, G adapted from Grimshaw (2018)

be expected in gold particles in their original hypogene setting. In such undeformed grains, twin boundaries are common and straight (Fig. 4B). Their presence has been ascribed to post-precipitation annealing, which requires temperatures of > 300 °C (Hough et al. 2009). Not all grain boundaries are twin boundaries, identifying the particle as a cluster of grains (Fig. 4B, grain 1), and curved or convoluted grain boundaries often appear associated with chemical variation (Fig. 4C).

Distinct grain characteristics revealed by EBSD and particular types of compositional heterogeneity have been observed, e.g., the numerous fine-grained domains in Au-rich rims of gold particles (Stewart et al. 2017), and coincidence of compositional variation and grain boundaries (Hough et al. 2009). Here, we show three fundamentally different relationships between grain boundaries and compositional heterogeneity in gold-particle cores. Alloy variation associated with grain boundaries is not only seen by increased Au content as

described by Hough et al. (2009) but also by presence of thin Ag-rich films (Fig. 1F; henceforward "tracks" following the terminology of Leake et al. 1992), there are two variations of these: one in which variations are symmetric away from the grain or twin boundary (Fig. 4C; red and blue arrows), and a second in which they are asymmetric relative to the grain boundary, comprising oscillating Au- and Ag–rich alloy zones (Fig. 4C; black arrows). Alternatively, the change of alloy chemistry is independent of a grain or twin boundary (area r, Fig. 4E, F).

Transport of gold particles within the fluvial environment results changes in orientation within individual grains. The placer-gold particle shown in Fig. 4G exhibits a curved twin boundary (site 1) and clear orientation changes, i.e., lattice distortions within individual grains (Fig. 4G, site 2). In addition, some detrital particles may exhibit small grains with distinct oscillatory Au–Ag zones at their edge (Fig. 4H).

## Chemical and mineralogical characteristics

### Internal compositional characteristics of natural gold alloys

Alloy heterogeneity within a sample population may manifest itself as different compositions of homogeneous particles or as heterogeneity within individual particles (Fig. 1A, B). Intra-particle alloy heterogeneity takes various forms, some of which have been described above in relation to Figs. 1A and 4B–E. A variety of other microfabrics caused by Au–Ag variation has been observed in gold particles from many different localities and these are described below.

Heterogeneity with respect to Au and Ag is by far the most common alloy variation. The distinct character of the Au-enriched, or equivalently, Ag-depleted rim is evident in BSE imaging (Fig. 1C), and often during optical examination, due to its rich orange–yellow color. Rims are typically 2–10 μm in true thickness and comprise alloy of > 98 wt.% Au (Knight et al. 1999b), occasionally containing inclusions of other minerals either entirely within, or straddling the rim–core interface (Fig. 1D). Internal alloy heterogeneity may take the form of areas of clearly differing composition (Fig. 1A), or as more subtle compositional differences (Fig. 1E). Thin well-defined tracks that are relatively rich in Ag can be observed in the gold particles illustrated in Fig. 4C, (area 1, red arrow) and Fig. 1F (site 1). Adjacent tracks of Ag- and Au-rich alloy are regularly encountered (Fig. 4C, areas 3 and 4 black arrows, and Fig. 1F,area 2). Systematic polygonal zonation that is sympathetic to grain boundaries has also been described above (Fig. 4c, D), and is sometimes adjacent to an unaltered portion of a particle (Fig. 1G). In some cases, this microfabric is overprinted by Au-rich tracks that partially infill cracks coincident with grain boundaries (Fig. 1H).

Localized concentrations of other minor alloying elements also occur as patches or tracks. Elevated Cu contents in Au–Ag alloy may present as concentric zoning of Au–Cu– intermetallics, surrounding a Au–Ag core (Fig. 1I), or as patches of relatively Cu-rich alloy (Fig. 1J). Exsolution of tetra-auricupride (AuCu) from Au–Ag alloy has been reported by Knight and Leitch (2001) in gold from various localities in British Columbia. Figure 1K shows a relationship between the Ag content of the host alloy and the development of exsolution microstructures. The polygonal pattern of heterogeneity in Au–Ag (shown in Fig. 1G and H) may also be caused by variation in Cu–Ag–Au (Fig. 1L).

Gold containing relatively high Hg and Ag is a component of some sample populations, where it may form entire particles, or late-stage alloy in heterogeneous particles (Chapman et al. 2006, Chapman and Mortensen 2016). In gold from alkalic porphyry systems, Hg-rich Au-Ag alloy may also be associated with Pd (Fig. 1M and Chapman et al. 2017). Intra-particle heterogeneity with respect to Hg was investigated by Chapman et al. (2010a) in an EPMA study that used a long counting time to lower detection levels to around 0.1 wt.%. Traverses of polished sections of some gold particles from the Yukon showed variable Hg contents of 0.1 wt.% (~LOD) to around 0.3 wt.%, without a corresponding change in Au/Ag ratio; a subtle variation that is not observable in BSE imaging.

### Compositional ranges of alloys and style of mineralization

The extensive database available to this study has permitted a comprehensive comparison study of the ranges of Ag values in individual sample populations, but parallel considerations of Cu, Hg, and Pd are not possible owing to variation between different studies in the protocols for measuring and reporting these elements. In addition, the concentration ranges of Cu, Hg, and Pd in sample populations are often low, straddling the limit of detection for EPMA. While these data sets do not constitute a robust quantitative resource applicable to all sample populations, in many cases, minor metals are clearly detectable and form an important component of a signature. Table 1 presents key features of alloy signatures for gold from the various styles of mineralization.

Figure 5A compares the mean Ag contents across broad styles of gold mineralization, using data in Online Resources 1–3. While there is significant overlap in terms of Ag contents in gold from orogenic and magmatic-hydrothermal systems, oxidizing chloride hydrothermal systems are generally identifiable by Ag values of < 5 wt.% often accompanied by measurable Pd (Chapman et al. 2009). Further differentiation between orogenic and magmatic-hydrothermal systems according Ag ranges of individual source styles is depicted in Fig. 5B. A comparison of our data with that from Morrison et al. (1991) shows a broad similarity in the range of Ag contents according to style of gold mineralization. Gold from Precambrian orogenic systems exhibits lower Ag values than that from Phanerozoic orogenic systems, but both ranges

**Table 1** Summary of information describing populations of gold grains from published (P) and unpublished (U) studies. Locations, references and summary compositional information are provided in Online Resources 1–3

| Style of mineralization | Localities | | | | No. particles (placer+lode) | | Main peographical extent | Compositional characteristics | | |
|---|---|---|---|---|---|---|---|---|---|---|
| | Lode | | Placer | | | | | Ag range wt (%) | Other metals in alloy wt% | Inclusion suite chemistry |
| | P | U | P | U | P | U | | | | |
| Orogenic, Precambrian | 12 | 1 | 11 | 35 | 1680 | 2276 | Zimbabwe, West Africa, East Africa, Madagascar, Finland | 5–50, but many <10 | Cu to 2 common<br>Occasional Hg to 3 | S,±As, ± (Te+Bi) |
| Orogenic, Phanerozoic | 50 | 1 | 218 | 110 | 20,578 | 8900 | UK and Irish Caledonides, Canadian Cordillera | 4–30 | Occasional Hg to 10 | i.S,<br>ii. S+As<br>iii.S+Te±As±Ag<br>iv. Pb+S+Sb±As |
| Low-temperature, oxidizing, chloride systems | 5 | 0 | 12 | 1 | 895 | 50 | Brazil, England, Scotland, Czech Republic | 0–13 | Pd or Hg to 12<br>Rare Cu to 4 | Se±Te+wide range of metals |
| Calk-alkaline porphyries and associated epithermal | 6 | 0 | 12 | 0 | 1326 | 0 | Canadian Cordillera Indonesia, Chile | | Cu usually >0.05 | Bi+Pb+Te+S |
| Alkalic porphyry Cu-Au±Mo mineralization | 4 | 0 | 6 | 3 | 809 | 183 | Canadian Cordillera, | 5–40 | Hg, Pd to 11 in around 4% of particles | Hg+Pd+Pb+Bi+Te+Cu |
| Low- to intermediate-sulfidation epithermal mineralization | 2 | 0 | 19 | 5 | 1570 | 284 | Canadian Cordillera, Scotland | 1–50 | Occasional Hg to 10 | S, ±As,+Te,+Ag, Bi, |
| High-sulfidation epithermal mineralization | 2 | 0 | 1 | 1 | 112 | 99 | Fiji, Bulgaria | 1–14 | Cu to 1 | Cu+Pb+Zn+S+As±Te |
| Skarn mineralization | 0 | 0 | 1 | 0 | 175 | 0 | Ecuador | Insufficient data | | |
| Unclassified magmatic hydrothermal systems | 0 | 0 | 6 | 0 | 293 | 0 | Ecuador, Scotland, N. Wales, Bulgaria | Insufficient data | | |
| Placer samples comprising gold from orogenic sources and low-temperature, oxidizing, chloride systems | 0 | 0 | 9 | 0 | 592 | 0 | Scotland, England | Gold from these styles of mineralization exhibits very different compositional characteristics. The values of statistical measures for sample populations would be mostly influenced by the proportion of gold particles from each style. | | |
| Unclassified | | | | 1 | | 7 | Sardis (Greece) | Insufficient data | | |
| Totals | 77 | 2 | 291 | 156 | 28,040 | 11,792 | | | | |
| | 79 | | 447 | | 39,832 | | | | | |

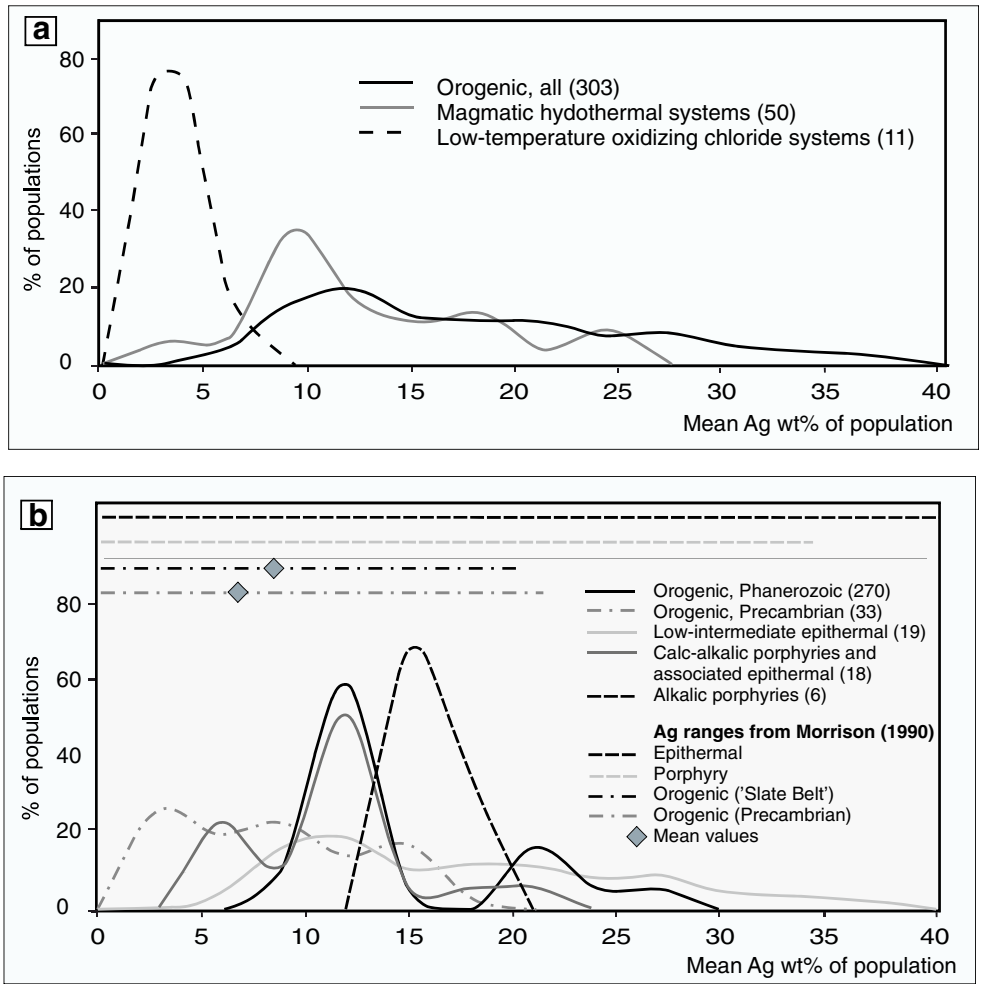


**Fig. 5** **a**: Mean wt.% Ag values for populations of gold particles from orogenic, magmatic-hydrothermal and oxidizing chloride-hydrothermal systems. **b**: Mean wt.% Ag for more refined source styles of orogenic and magmatic-hydrothermal mineralization. Dotted lines indicate the mean values for Ag ranges of gold from orogenic settings and ranges of values in gold from porphyry and epithermal (0–44 wt.% Ag) systems (data from Morrison 1991). Figures in parentheses refer to the number of populations in each curve (data from Online Resources 1 and 2)

encompass the mean Ag wt.% values of gold from magmatic-hydrothermal systems.

Copper is rarely an important alloy component in gold from Phanerozoic orogenic gold systems (Moles et al. 2013), but it is normally detectable in gold from several other settings. Gold from some African localities in granite-greenstone terranes consistently shows Cu values measurable by EPMA (Dongmo, 2018; Omang et al. 2015). Elevated levels of Cu have also been reported in gold derived from ultramafic rocks (Knight and Leitch 2001; Zaykov et al. 2016; Oberthür et al. 2017).

Minor alloying elements can provide useful discriminants to characterize gold populations where at least one of two criteria is fulfilled. In some cases, most gold particles exhibit detectable, but low, typically < 1 wt.% concentration values, e.g., Cu in gold from porphyry systems (Chapman et al. 2017, 2018). In other cases, sporadic higher concentrations are observed, for example Hg values of ≤ 12 wt.% in gold from some orogenic systems (Knight et al. 1999a; Chapman et al. 2000a, 2010b, Chapman and Mortensen 2016). Palladium values up to 4 wt.% have been reported in gold from late-stage veins in alkalic porphyry-epithermal systems (LeFort et al. 2011; Chapman et al. 2017), and some gold particles from oxidizing chloride hydrothermal systems comprised 12 wt.% Pd (Leake et al. 1991; Chapman et al. 2009). Palladium-bearing gold has been reported from several localities in Brazil, where redox-controlled processes are advocated (Olivo et al. 1995; Cabral et al. 2002a, b, 2008a; Galbiatti et al. 2009).

## Trace-element distribution within gold particles

A total of 1100 gold particles that were characterized by EMPA were subsequently analyzed using a laser-ablation-quadrupole-ICP-MS system (details in Online Resources 1–3). Selection of gold particles from different styles of mineralization has permitted the evaluation of which elements might find use as generic discriminators. A suite of 33 elements were considered, and Fig. 6A shows the proportion of gold particles in which each element was recorded above the LOD. Ag, Au, Cu, and Hg are sufficiently common to form generic discriminants and the quality of the Cu and Hg data is far superior to that obtained from EPMA. Regarding other elements, only Hg, Cu, Sb, and Bi were observed in over

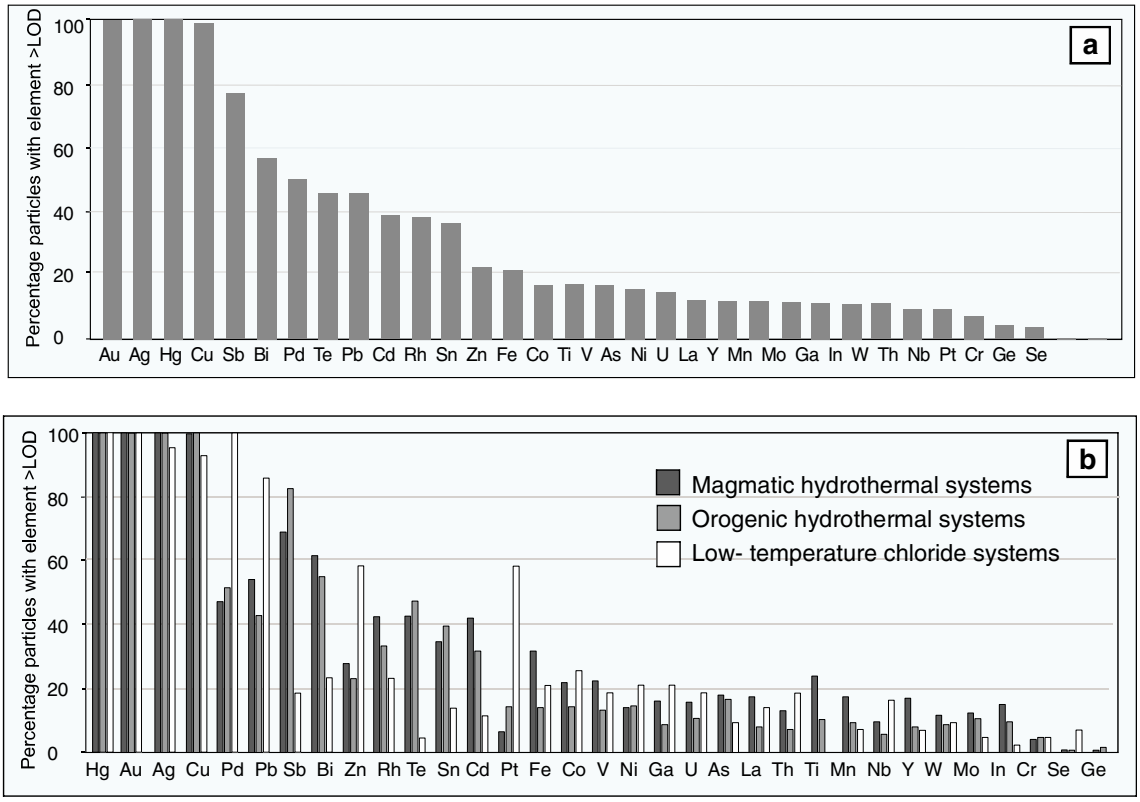


**Fig. 6** Abundance of elements at trace level in a study of 1100 gold particles by quadrupole-LA-ICP-MS. **a**: Element abundance in entire population, **b**: comparison of element distribution according to hydrothermal system

50% of the ablated gold particles. A further suite comprising Pd, Pb, Te, Rh, Sn, and Cd was present in between 35 and 50% of gold particles, while the remaining elements all returned abundances of below 25%. Where elements are observed at trace levels, their concentrations often vary considerably between analyses. Of the thirteen most common elements (excluding Au and Ag), seven exhibited standard deviations larger than the mean values. Elemental abundancies at trace levels have also been examined in terms of the style of mineralization (Fig. 6B). Gold from magmatic-hydrothermal and orogenic environments show similar elemental abundances, but Pd, Pb, Zn, and Pt are present in a higher proportion of gold particles formed in low-temperature chloride systems.

In this reconnaissance study, we have selected gold particles from an alkalic porphyry setting and two unrelated orogenic systems in order to explore the distribution of elements at the trace level. Figure 7 A–K shows major and trace-element maps of two different gold particles (particle 1: Fig. 7A–C and particle 2 Fig. 7D–K) from the Similkameen River, British Columbia, Canada, a former placer mining region adjacent to the Copper Mountain alkalic Cu–Au porphyry (Chapman et al. 2017). The elements chosen for depiction in Fig. 7A–D are those that are routinely analyzed by EPMA. Contrasting patterns of internal Ag distribution are seen in particle 1 (homogenous distribution; Fig. 7A) and particle 2 (heterogeneous distribution; Fig. 7D). The distribution of Hg in particle 1 conforms to two broadly concentric zones, and in general, the distribution of Cu appears antipathetic, but the degree of heterogeneity appears greater. Particle 2 shows widespread Pd at trace level (Fig. 7E), but this does not always correlate with Ag (Fig. 7D). Heterogeneity due to inclusions and trace element association within them in particle 2 is illustrated in Fig. 7 F–J. Pyrite inclusions that were identified during SEM screening are spatially coincident with traces of Bi (Fig. 7G) and all lanthanides, although only La is shown here (Fig. 7 H). However, not all pyrite inclusions exhibit the same trace-element signature, and Fig. 7I shows that only one contains Pb. Small areas of elevated Cu content (Fig. 7J) are not correlated with Fe, Pb, or Bi (Fig. 7F, G, I), and indicate the presence of a different mineral type that was not observed during visual screening for inclusions. Taken together, these figures show that inclusions exhibit trace-element signatures different from the host alloy, but that the nature of that signature can vary between different inclusions of the same mineral. Figure 7K–O shows highly localized, but low-intensity element responses in gold particles from three localities. In most cases, the distribution of the elements depicted does not coincide and no clear correlations were observed with other elements studied (but not shown here). The observation of this pattern of heterogeneity in all gold particles studied suggests that their presence is widespread and is consistent

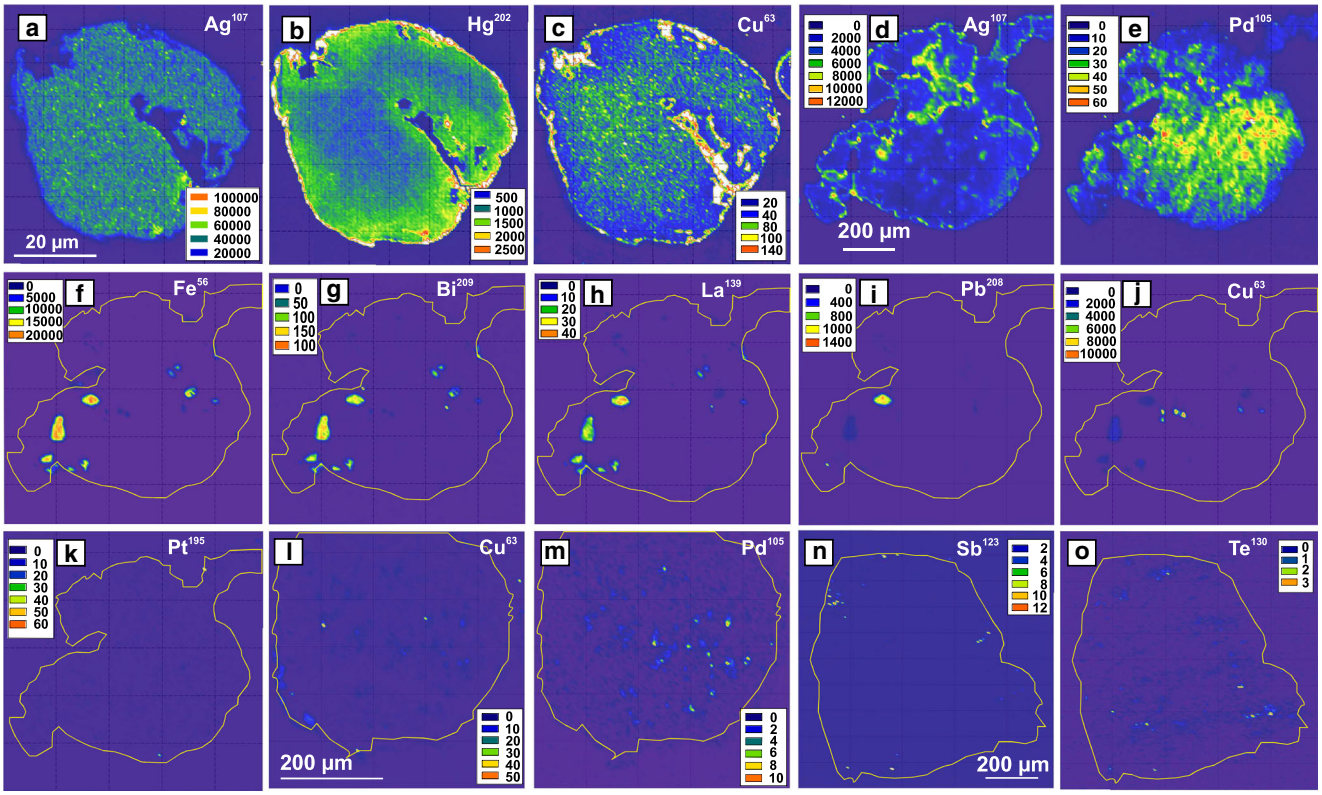


**Fig. 7** Examples of heterogeneity in maps generated by LA-ICP-(ToF)MS. **a**–**d** and **e**–**k**: Gold particles from the Similkameen River, BC, Canada. **l**, **m**: particles from Cunningham Creek, BC, Canada. **n**,**o**: gold particles from Eldorado Creek, Yukon, Canada. **a**–**e**: examples of heterogeneity in elements normally detectable using EPMA. **f**–**j**: trace element distribution in mineral inclusions. **k**–**o**: localized concentrations of specific elements above background levels ('clusters'). Color keys indicate signal responses corresponding to different intensities in different images. In each case, the associated numerical key is the measured signal intensity and a qualitative indication of concentration

with high degrees of variation for some elements recorded using the quadrupole-MS system and reported above. Such heterogeneities highlight why ToF systems may be favored over conventional quadrupole spectrometers.

## Mineral inclusions

Inclusions are manifestations of the vein mineralogy (Fig. 8C) and are inherited by detrital particles (Fig. 8D–N). Their presence in detrital gold particles was noted by Boyle (1979) and several subsequent studies (e.g., Loen 1994, 1995; Youngson and Craw 1995; Knight et al. 1999a). The first systematic recording of inclusions suites in sample populations was undertaken by the British Geological Survey (BGS), where inclusion assemblages of placer particles were employed to reconstruct the mineralogy of the eroded source, and hence develop a deposit model (Leake et al. 1991, 1992). In general, inclusion suites have proved a valuable source of information for placer-lode studies, and particularly for defining signatures that are diagnostic for the style of mineralization (Chapman et al. 2017, 2018). A summary of inclusion chemistry relating to source style of mineralization is included in Table 1.

At any locality, the inclusion suite reflects the coeval ore mineralogy. Consequently, pyrite is often the most common inclusion (Fig. 8D), but there are frequently contributions from other common primary ore minerals, such as chalcopyrite (Fig. 8E). Gold particles may contain multiple inclusions of the same mineral (Fig. 8D, F), or inclusions of more than one mineral (Fig. 8G). In addition, a wide variety of more unusual mineral species have been recorded, such as niccolite (NiAs; Fig. 8F). In some cases, inclusions are heterogeneous (Fig. 8H, I), in others they appear fractured (Fig. 8J) and infilled by alloy with the same composition as the inclusion host.

Inclusions of "non-ore" minerals such as silicates and carbonates are also observed. Quartz is the most common inclusion, although carbonates are present in gold particles from many localities (Fig. 8J). Phosphate inclusions, such as monazite and apatite (Fig. 8K), occur sporadically. In general, the information from these non-ore minerals is not as useful as that from ore minerals. However, mineral chemistry can help to constrain conditions of formation, e.g., V and Cr content of magnetite inclusions (Dongmo et al. 2018). In some cases, non-ore minerals can be used to suggest or exclude particular mineralizing environments, e.g., the presence of carbonates is incompatible with a high-sulfidation epithermal source. Inclusions of some silicates may reflect the lithology of the country rock. For example, Fig. 8M shows an amphibole

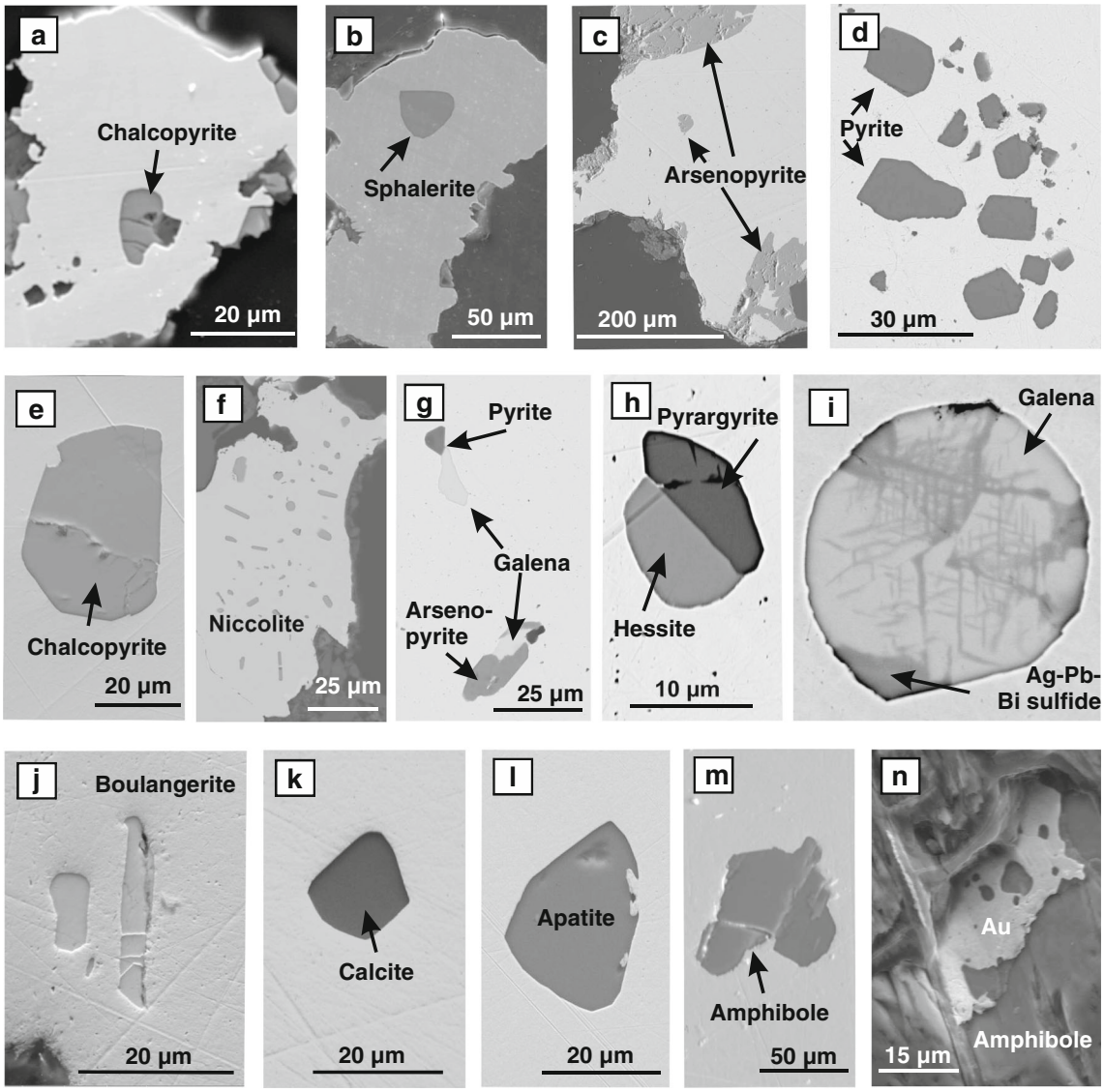


**Fig. 8** Examples of mineral inclusions. All SE images. **a**–**c**: Gold particles that have been directly liberated from ore **a**: (Mount Polley, British Columbia, Canada). **b**: (Lone Star, Klondike, Yukon, Canada). **c**: Relationship between vein mineralogy and inclusions (Bralorne Mine, British Columbia, Canada). **d**–**l** Inclusions within detrital gold particles: **d**: Thistle Creek, Yukon, Canada. **e**: Orange River, Namibia. **f**: Spruce Creek, British Columbia, Canada. **g**: Dolly Creek, Victoria, Australia. **h**: Blueberry Creek, Yukon, Canada. **i**: Sixtymile District, Yukon, Canada. **j**: Boulangerite showing fractures, Independence Creek, Yukon Canada, **k**: Glen Lednock, Scotland. **l**: Serra Pelada, Brazil. **m**, **n**: Lake Turkana, Kenya

inclusion in a detrital particle from Lake Turkana, Kenya. Another particle from the same location exhibited an intimate association between gold and host amphibole (Fig. 8N). Similarly, clinopyroxene and garnet inclusions have been found in gold from skarn deposits in Ecuador, providing a clear indication of the gold source (Potter and Styles 2003).

In addition to characterizing alloy compositions of gold particles, LA-ICP-MS systems can also be used to determine trace element concentrations in mineral inclusion species. The application of trace-element chemistry of mineral inclusions was explored during the present study, using a quadrupole-LA-ICP-MS system. Trace-element signatures of 10 pyrite inclusions and 7 galena inclusions in placer gold particles from Sutherland, Scotland, showed that siderophile elements partition strongly to pyrite, whereas Se, Cd, Bi, and Sb reside in galena (Fig. 9).

Figure 10A combines data sets from Online Resource 1 to show the range of abundances of inclusions in all populations studied. Inclusions are revealed in less than 1 in 10 polished sections in approximately 60% of cases. Figure 10B compares inclusion abundance with the source style of the mineralization, for populations that contain 20 or more gold particles. Most styles of gold mineralization contain a range of inclusion abundances, but the incidence of inclusions in Precambrian orogenic samples generally appears lower than in the other sample sets.

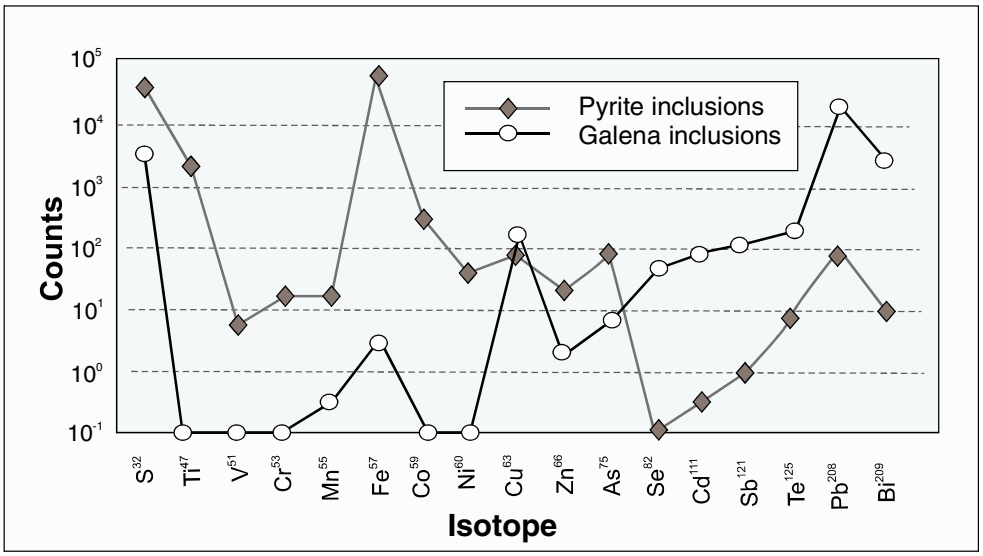


**Fig. 9** Quadrupole LA-ICP-MS measurements showing partitioning of different elements to different inclusions within detrital gold from the same locality

## Discussion

### Nature of heterogeneity at trace-element levels

Banks et al. (2018) reported compositional characteristics of gold from orogenic and alkalic porphyry settings in British Columbia (BC), using a quadrupole-LA-ICP-MS system. The present study has drawn upon this data set and the results of other analyses of gold from localities in Yukon and Scotland (details in Online Resources 1–3) to show that, in general, trace-element concentrations and distributions are highly variable. The data sets available to this study show that Au, Ag, and Hg are ubiquitous, and that Cu is absent only in some particles formed in a low-temperature chloride hydrothermal system (Fig. 6). Sporadic abundance of other elements reduces their potential as generic discriminators, although specific studies may be able to exploit the locally common occurrence of elements such as Pd, Sb and Bi.

Some large spikes in Fe values are accompanied by anomalous concentrations of siderophile elements, indicating the ablation of subsurface inclusions. However, the causes of more subtle responses of single or small numbers of elements can only be interpreted with confidence in the light of results gained using the ToF-MS system. It is now clear that minor elements can be present in some gold particles as alloy components, whereas in others their presence is highly heterogeneous (compare Pd distribution in Fig. 7E and M). Inclusions are clearly visible in quadrupole-LA-ICP-MS responses, and imaging using the ToF-MS system may show a trace-element signature in inclusions distinct from the host alloy (Fig. 7F–J). The elements Cu, Ag, Hg, Sb, and Pd may be present as inclusions within an alloy that may or may not contain that element as an alloy component. Localized low concentrations of specific elements which do not correspond to stoichiometrically defined minerals are common, and henceforward these features are referred to as "clusters."

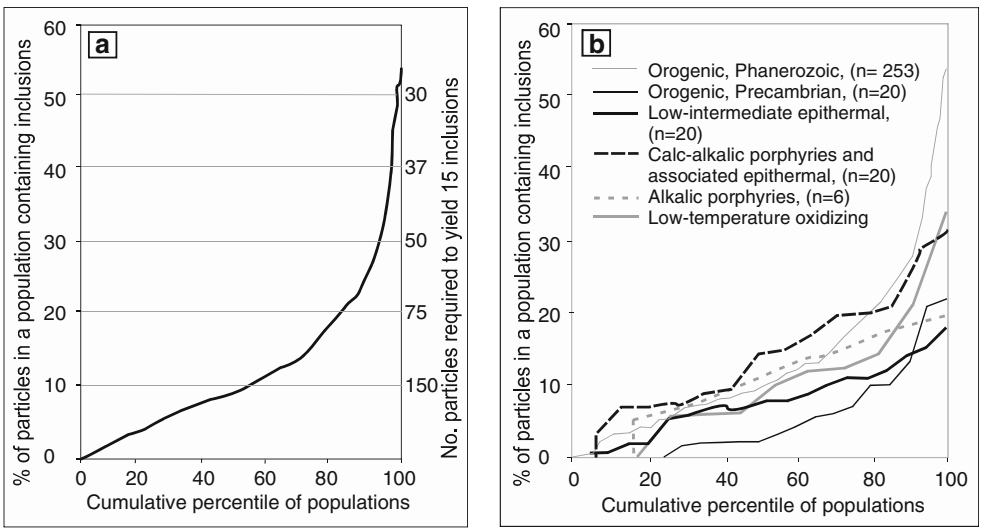


**Fig. 10** Inclusion abundance in populations of gold particles (data sources are described in Online Resource 1 and 2). **a**: Inclusion abundance of the whole data set ($n = 323$ populations of >30 particles). **b**: Inclusion abundance according to style of mineralization

The presence of trace-elements within mineral inclusions was reported by Banks et al. (2018) using both approaches to LA-ICP-MS and has been confirmed by the present study. A pilot study included in the present paper is the first systematic characterization of trace-elements in multiple inclusions from the same sample population. This approach has demonstrated the detailed information that can be obtained regarding the partitioning of individual elements to specific mineralogical hosts during precipitation, and is a hitherto unreported aspect of trace element chemistry of gold particles.

Finally, the limited number of elements that exhibit homogenous distribution within gold alloy differs from those historically reported as minor alloy components. For example, Boyle (1979) identified Fe as a common minor alloying element, and listed over 40 other metallic elements which could be present in trace amounts. It now seems clear that the presence of most elements within native gold is a consequence of extreme heterogeneity in the form of inclusions or clusters. Bulk analysis of gold, for example by whole-particle digestion, takes no account of mineralogical heterogeneity and has resulted in widely held misconceptions on the chemical nature of natural gold alloy.

## Causes and timing of chemical heterogeneity within gold particles

Different microfabrics commonly observed in gold particles are formed by processes active in specific environments. We address these in terms of three categories that relate to the timing of their formation: (i) primary precipitation from hydrothermal fluids; (ii) modification of pre-existing alloy while resident in the original host but isolated from surficial processes; and (iii) modification of particles in the surficial environment.

### The effect of the conditions of primary precipitation

Gammons and Williams-Jones (1995) considered the chemical equilibrium that describes precipitation (Eq. 2), identifying the parameters that control the Au–Ag composition of precipitated gold alloy:

$$Au_{alloy} + AgCl_2^- + 2H_2S_{(aq)} = Au(HS)_2^- + Ag_{alloy} + 2Cl^- + 2H^+ \quad (2)$$

Increasing $Ag_{alloy}$ is associated with decreasing temperature (via the equilibrium constant), decreasing $Au/Ag_{aq}$, increasing pH, decreasing $aCl^-_{(aq)}$ and increasing $aH_2S$. Most of these parameters are expected to change during the evolution of a mineralizing hydrothermal system, with some concurrent changes; e.g. decreasing $aH_2S$ and falling temperature having contrasting effects on the value of $Au/Ag_{alloy}$. Stable mineralizing conditions (in terms of P–T–X) should generate a population showing inter- and intra-particle homogeneity. However, homogeneous particles from the same population often exhibit different Ag contents (Fig. 1B), suggesting very stable local conditions of precipitation with either spatial or temporal variation in P–T–X conditions, during a single mineralizing event.

Some compositional characteristics, involving other alloy components, can also be ascribed to the primary environment of precipitation. The temperature dependence of Cu in Au–Ag alloy was proposed by Antweiler and Campbell (1977), a hypothesis that is supported by observations of relatively high Cu concentrations in gold from magmatic-hydrothermal systems (Morrison et al. 1991; Chapman et al. 2017, 2018; Gas'kov 2017). Chapman et al. (2010a) examined the controls on Hg in Au alloy,but did not identify a robust generic relationship between the conditions of mineralization and the alloy composition. Lower temperatures favor higher Ag contents in Au–Ag alloys (Gammons and Williams-Jones 1995), and the high volatility of Hg could result in later incorporation into minerals and preferential deposition at lower temperatures (as suggested by Gas'kov 2017). Conversely, the Hg content of Au–Ag alloys from various vein systems in the Otago Schists, New Zealand, was independent of depth of emplacement (and presumably corresponding temperature) at depths from 2 to 6 km (Mackenzie and Craw 2005). Gold containing Hg has also been reported from Archean paleoplacers in southern Africa (Von Gehlen 1983), and Brazil (Koglin et al. 2012). The presence of Pd-bearing gold in low-temperature oxidizing chloride hydrothermal systems results from co-transport of Au and Pd as chloride complexes (Mountain and Wood 1988). Mechanisms of Pd fractionation into the fluids responsible for Pd-bearing gold alloys that are found in late-stage veins in alkalic porphyry systems remainunclear, as both chloride and sulfide complexes may be involved.

The occurrence of minerals such as quartz (Fig. 3A) on the outside of gold particles provides an indication of the lode mineral associations. Some gold particles exhibit surface coatings of minerals which are either mechanically or chemically unstable in surface environments, indicating proximity to source and likely recent liberation. In addition, specific minerals may be suggestive of specific ore-forming processes. For example, the common occurrence of mm-scale Bi telluride on numerous gold particles from Mechanic Creek, Yukon (Fig. 3B), provided evidence for gold formation through a BiTe-collector process (Chapman et al. 2018).

The intimate relationship between most sulfide-mineral inclusions and host gold particles strongly suggests that they are coeval. The well-defined shape and size of mineral inclusions (relative to the host gold particle; Fig. 8A and B)

preclude their formation through exsolution from the gold alloy. The presence of silicate inclusions may be due to gold enveloping adjacent gangue minerals during initial precipitation, as shown by amphibole inclusions (Fig. 8M). Silicate inclusions situated near the periphery of gold particles may have been emplaced by impact during transport, but the presence of voids in the gold alloy surrounding such "inclusions" readily distinguishes them from those that are coeval with gold.

There is no generic relationship between the incidence of elements in inclusion suites and their occurrence as trace components within gold alloys (Fig. 6A). For example, Fe was detected in only 20% of ablated gold particles, and As in 17% but pyrite and arsenopyrite are the most commonly encountered inclusion species. Of the major mineral classes, selenides are the most uncommon contributors to inclusion suites, but where present they may be dominant. The bonanza-style mineralization of Minas Gerais and Serra Pelada, Brazil, shows a clear Au-Pd-Se association (Cabral and Lehmann 2007) that demonstrates the potential for strong, but atypical element relationships on a deposit scale. In general, inclusion suites correlate to ore mineralogy which underlines their use as indicators of the source style of mineralization of detrital gold particles.

It seems likely that the formation mechanism of the small mineral inclusions and element clusters that are identified by LA-ICP-(ToF)-MS would be similar to that of their larger counterparts, although the range of elements represented appears to be greater than has been detected in larger inclusions identifiable by SEM. At present, the mechanisms responsible for producing such clusters remain unclear.

### Post-depositional modification: hypogene environment

For studies whose objective is to use gold composition to deduce conditions of mineralization, it is clearly important to establish whether or not heterogeneous features are related to the ore-forming stage. Disequilibrium between pre-existing gold particles and the surrounding fluid has been invoked to explain heterogeneous alloy microfabrics in a study of gold from the Borland Glen locality, Scotland (Chapman and Mortensen 2016), where many gold particles have been extensively modified by replacement of the primary alloy with a Ag-rich alloy. Increased Ag values (Fig. 4E) are associated with wittichenite ($Cu_3BiS_3$) and hessite ($Ag_2Te$) inclusions and do not correspond to grain or twin boundaries identified by EBSD (Fig. 4F). This microfabric can be explained by an interfacial coupled dissolution–replacement reaction (Putnis 2009), driven by a fluid in chemical disequilibrium with the original gold particle. Parallel bands of Au-Ag alloys of different compositions (Fig. 4E, area r) can be ascribed to fluid changes during the replacement reaction (e.g., Spruzeniece et al. 2017), and the overall increase in Ag may be a consequence of temperature reduction (Gammons and Williams-Jones 1995). This sample population shows two features through which timing of alloy modification may be deduced. Firstly, the effect was widespread within the primary mineralization, as indicated by replication of replacement microfabrics in many placer gold particles. Secondly, Au was not completely stripped from the pre-existing particles, so the fluid contained some $Au_{(aq)}$. These conditions appear more compatible with evolution of the primary mineralizing environment than a later, unrelated hydrothermal event.

Fluid that enters a polycrystalline particle along grain boundaries, at post-depositional conditions, may induce replacement reactions that occur perpendicular to the grain boundary, in the grains adjacent to the boundary (e.g., grains 1&2—blue arrows, Fig. 4C). Twin boundaries are crystallographically controlled and low-energy sites, therefore "tighter" to fluids, although in some cases, minor replacement reaction may occur along twin boundaries that are deformed (e.g., red arrows, Fig. 4C).

Heterogeneous microfabrics observed in gold (Fig. 4H) may be formed in other minerals such as zircon (Piazolo et al. 2012), and chromite (Satsukawa et al. 2015) in response to local high degrees of deformation at grain edges. The physical impact of hard material against the detrital gold particle induces locally high dislocation densities (e.g., Piazolo et al. 2012). In the presence of a fluid, new grains may nucleate at such sites of high stored energy, growing in chemical equilibrium with that fluid to produce distinct bands of variable composition corresponding to successive boundaries of new grain growth (black arrows, Fig. 4H). This mechanism was advocated for the over-thickened Au-rich rim formation of detrital grains (Stewart et al. 2017).

If deformation is less severe, with neighboring grains exhibiting different dislocation densities, strain-induced grain boundary migration may occur. Free energy may be lowered in any system with monophase grain boundaries, i.e., polycrystals/grain clusters of gold, where the total grain boundary area and internal strain energy are reduced. This process ultimately consumes some of the original grains and results in a larger average grain size. In addition, if the fluid that is present during grain growth is distinct from the formation fluid, then migrating boundaries may exhibit a chemical signature in equilibrium with that fluid (Piazolo et al. 2010). The resulting compositional variation indicates the direction of grain boundary migration and is present on one side of the original boundary only i.e., chemical variation is asymmetric with respect to the present-day grain boundary. The presence of several parallel compositional zones reflects temporal migration associated with different fluids and/or evolving fluids (Fig. 4C, D, black arrows). Similar compositional

variation has been observed in zircon (Piazolo et al. 2012), and in the trace-element content of quartz (Lind 1996; Holness and Watt 2001, Bergman and Piazolo 2012; Morgan et al. 2014). This feature is rare in gold particles, and has only been observed in a few particles from a small number of populations. Therefore, the criteria for formation must only be fulfilled occasionally, which may be related to the availability of fluid during residence post-ore- forming stage. Compositional variation is usually confined to Au–Ag, but Fig. 1I shows modification to a Au–Ag–Cu primary alloy with auricupride (AuCu), indicating that the later, reactive fluid was relatively Cu-rich.

In addition to replacement reactions and grain-boundary migration, diffusion along dislocation arrays within deformed grains may induce a local change in trace-element content (Piazolo et al. 2016). These then result in a combination of distinct changes in trace elements along subgrain boundaries, and more "nebulous" chemical changes within highly distorted areas internal to the grain (Fig. 1E, black arrow points to subgrain boundary; e.g., Piazolo et al. 2012; Chapman et al. 2019).

While replacement of a large proportion of original Au alloy by more Ag-rich metal is probably indicative of evolving conditions within the mineralizing system, heterogeneity spatially related to grain boundaries may form later. In both cases, the Au alloys formed later in the paragenesis are relatively Ag-rich. According to the controls of Au/Ag ratio in the gold alloy described by Gammons and Williams-Jones (1995), increased Ag content is a consequence of lower temperatures and/or the lower Au/Ag ratio of the modifying fluids, with respect to the initial Au mineralizing fluids, i.e., conditions consistent with the hypothesis of paragenetically late (and hence lower-temperature) modification.

Some inclusions appear to exhibit fractures, infilled by the gold matrix (Fig. 8J). These may result from stress regimes in the post-depositional environment (Cabral et al. 2008a, b), although future EBSD studies of such particles may prove informative. Inclusions that comprise two or more mineral species are most likely a consequence of post-depositional re-equilibration. These are common in the Au–Ag–Te–S ± Fe-mineral system (Fig. 8H), but also occur more generally in other systems where several elements are present. Exsolution microfabrics within inclusions (Fig. 8I) have only been observed in minerals of the Pb–Ag–Bi–S system.

### Post-depositional modification: surficial environment

There is a consensus that Au-rich rims are formed in the secondary environment. However, opinions differ on whether these features are caused by Ag depletion (e.g., Groen et al. 1990), or by Au augmentation, through the accumulation of the approximately 1 μm pure Au crystals and buds that have been reported on the surface of gold particles by many workers (e.g., McCready et al. 2003, Reith et al. 2018). True thicknesses of rims are generally similar (1–10 μm) irrespective of particle size (Knight et al. 1999b). This observation suggests a generic control to their formation and is likely more consistent with diffusion-controlled Ag removal than Au augmentation (Groen et al. 1990). Inclusions of ore minerals that are unstable in the surficial environment have been observed in rims, or straddling the core–rim interface, of several particles from the Canadian Cordillera, UK Caledonides, and Namibia (e.g., Fig. 1D). This feature, when coupled with the common limit to rim thickness, leads us to support a generic mechanism of rim formation by Ag removal. We acknowledge the general presence of minor overgrowths of secondary gold (Fig. 3I), but have seen no evidence that gold accumulation is progressive beyond these features. Consequently, we concur with Stewart et al. (2017) and Craw et al. (2017), who made a clear distinction between surface authigenic gold and a pre-existing rim formed by Ag depletion.

Nevertheless, in some placer localities in New Zealand and Yukon, gold particles exhibit much thicker rims. Stewart et al. (2017) explained the presence of relatively thick (> 100 μm apparent thickness) Au-rich rims in some New Zealand gold particles in terms of recrystallization, in response to physical deformation associated with gold-particle transport during successive fluvial downcutting events in a tectonically active region. Examples of crystallographic response to physical deformation during fluvial transport are illustrated by Fig. 4G, where the curved twin boundary and varying orientations, as shown by color variation, are interpreted to result from impacts within mobile sediment. An association of particle deformation with progressive surface composition modification may explain the presence of rims of 40–50 μm thickness in gold from Hunker Creek, Yukon, where the current river channel has reworked paleo fluvial sediments (Chapman et al. 2010b).

Au-rich tracks (Fig. 1F, H) are commonly observed in gold particles from both near-surface hypogene and placer settings worldwide (Knight et al. 1999a; Hough et al. 2009; Hancock and Thorne 2011). Modification of the initial gold alloy to yield Au-enriched areas could occur either in the late stages of the hypogene systems, or in the surficial environment. The Au content of Au–Ag alloy increases with temperature of precipitation and the ratio of Au/Ag in the fluid (Eq. 2). Scenarios in which either temperature increases and/or fluids become more Au-rich at the end of mineralization appear unlikely. Hough et al. (2009) considered both compositional and crystallographic evidence for gold-particle weathering by Ag removal along the fluid conduits provided by grain boundaries. The crystallographic orientations of the Ag-rich matrix and the Ag-poor track were the same, i.e., the absence of new crystal

domains indicated that gold had not been added to the system. Preferential removal of Ag is dependent upon the presence of surface fluids of neutral and mildly alkaline pH, where thiosulfate complexing facilitates both Au and Ag mobility (Webster and Mann 1984; Webster 1986), as opposed to acidic chloride fluids in which Ag is immobile (Krupp and Weiser 1992). In many cases, Au-rich tracks appear to partly infill voids (Fig. 1H), but in others, there is no observable porosity (Fig. 1F), meaning that the mechanism of Ag removal is unclear. The close spatial association of Au- and Ag-rich tracks (Fig. 1F) may be explained by exploitation of the same fluid conduit, at different times by different fluids, as suggested by Hancock and Thorne (2011).

## Description of natural gold as part of mineral paragenesis

Deposit-scale studies typically lack a systematic compositional study of gold particles, and paragenetic diagrams typically depict "gold" or "electrum" alongside otherwise sophisticated mineralogical characterizations. The understanding of the controls on Au–Ag ratio in gold alloy afforded by the study of Gammons and Williams-Jones (1995) facilitates the correlation of hypogene gold-particle composition with P–T–X constraints. Variation of gold-alloy composition in different paragenetic settings can be related to changes in various parameters, and consideration of the wider geological environment allows focusing on the most likely cause(s) of this change (e.g., Chapman et al. 2010a). Spence-Jones et al. (2018) showed how prevailing $fTe$ values influence the Ag content of Au alloy. These authors proposed that Ag initially formed hessite, until Te values were depleted, after which Ag values in Au–Ag alloy increased. Gold compositions have also been examined in terms of the complex stage-wise evolution of porphyry and porphyry-epithermal systems, both in terms of different stages of alteration (Palacios et al. 2001; Arif and Baker 2004), and also in terms of the porphyry-epithermal transition (Chapman et al. 2018). Characteristics of gold particles that are useful in interpreting paragenetic evolution persist into the placer expression, potentially providing an opportunity to predict the nature of the source mineralization, even in cases where the location is unknown.

## Design of future studies

### Analytical procedures

This study has demonstrated the rich information that can be gained through a combination of compositional and crystallographic approaches to the characterization of gold particles. For crystallographic studies, preparation of polished sections is a prerequisite. The validity of compositional characterization is dependent on analysis of the primary Au alloy whose location in heterogeneous particles is also only revealed in section. For this reason, it is not possible to characterize the alloy composition related to primary Au precipitation through whole-particle digestion, as some alloy compositions may have been formed in other environments. Additionally, the rim–core ratio of detrital particles changes with their size and shape, because maximum rim thickness is fixed in the absence of strain-induced recrystallization (Stewart et al. 2017). Neither is it possible to avoid sectioning by ablating through the Au-rich rim using a quadrupole-LA-ICP-MS system, given that the presence and nature of internal heterogeneity is unknown. Characterization of detrital gold particles through analysis of the surface is clearly inadmissible because of the rim.

A standard approach is beneficial, providing successive contexts for interpretation of the features observed at each stage. Initial BSE imaging, coupled with EDS analysis, provides a compositional and spatial overview of compositional heterogeneity and permits inclusion identification. Reflected-light microscopy could also find application here either if inclusions are to be analyzed by EPMA or if crystallographic information on minerals other than gold is important to the study. Subsequent investigations using EBSD can illuminate whether microfabrics are related to the ore-forming stage and can guide decisions on site selection for further in-depth spatially resolved chemical analysis.

Analysis of the primary alloy by EPMA involves selection of a site on the polished section chosen using the BSE-imaging facility of the instrument and, consequently, the analysis of a site free from alloy heterogeneity or inclusions is assured. This approach results in high levels of reproducibility in the alloy analysis for Ag, either when samples are reanalyzed on a different EPMA system (e.g., Chapman et al. 2000a), or when duplicate sample populations are collected and analyzed (Chapman et al. 2000b; Moles and Chapman 2019). Conversely, spatial variation in the concentrations of minor, but measurable components such as Cu, Hg, and Pd, as revealed LA-ICP- (ToF)MS imaging (Fig. 7b, c), is not evident from BSE images. In such cases, using the BSE image as a guide to analysis site does not guarantee generation of a representative value for minor elements. Nevertheless, analysis of populations of gold particles will generate a net result that indicates whether a minor alloying element is likely to be significant or not. Issues of accuracy at low concentrations are particularly acute where data manipulation involve artificially enhancing low values, such as in the production of ternary diagrams that show Au vs. (Ag × 10) vs. (Cu × 100) (e.g., Townley et al. 2003).

Most quadrupole-LA-ICP-MS systems rely on a light microscope to fix the positioning of the ablation pit, and

consequently informed selection of analysis site is not possible without prior characterization by SEM. Even if this information is available, it is impossible to predict possible compositional changes with depth that will be encountered during ablation. The use of trenching as opposed to pitting could partially alleviate this issue.

The application of LA-ICP- (ToF)MS systems to gold characterization is at an early stage, but the potential is clear. The capability to establish elemental co-variance both chemically and spatially combines the best outcomes of characterization by SEM, EPMA and quadrupole LA-ICP-MS systems. Elements may be assigned to their mode of occurrence, i.e., as alloy components, inclusions or clusters, in a way that is not possible with quadrupole-LA-ICP-MS systems. Furthermore, identification of all detectable elements is assured. As ToF instruments become more available to researchers, the approaches to gold characterization will also evolve, to accommodate the increased compositional and spatial information that is generated. Nevertheless, our ability to interpret data generated by quadrupole LA-ICP-MS in the context of gold-particle studies has been greatly enhanced by the understanding of spatial heterogeneity flowing from studies using the ToF-MS system.

### Numbers of particles required for robust characterization of a population

The number of particles required to characterize a population depends on the complexity and number of subpopulations present and the analytical techniques applied. Repeat sampling exercises have been undertaken (Chapman et al. 2000b; Chapman et al. 2010a: Moles and Chapman 2019), which have established that populations of around 30 particles are normally sufficient to characterize the Ag profile of a sample population using EPMA. Substantially more particles are normally required to characterize the inclusion assemblage, but that number varies according to mineralogical complexity and inclusion abundance. Ongoing work in this area suggests that 15 inclusions may yield useful data even where multiple mineral species are observed. The right-hand axis on Fig. 10A indicates the number of particles required to obtain 15 inclusions according to overall abundance in polished sections. For example, if 10% of sections reveal inclusions (i.e., the median abundance), 150 particles would be required. Figure 10B shows that gold from most styles of mineralization would generate a suitable sample in 50–60% of cases. Larger populations are clearly beneficial, but there may be practical reasons why obtaining this number may be problematic, for example gold scarcity at a specific locality or dependence upon donated samples. In addition, sample populations received from placer miners are rarely representative of the gold particle size range. This is not usually an issue regarding characterization of alloy compositions, but in our experience inclusion incidence is generally lower in smaller particles, particularly if they are flaky (Chapman and Mortensen 2016).

Trace-element heterogeneity has been identified in every individual gold particle irrespective of style of mineralization, and it is reasonable to assume that such heterogeneity is common, if not ubiquitous. This understanding must influence the interpretation of data generated by quadrupole-LA-ICP-MS systems. It is clear that the original aspiration to reduce the number of gold particles required to characterize a sample population through increasing the number of elemental discriminants cannot be fulfilled. Indeed, the range of elements detectable by LA-ICP-MS coupled with the potential for heterogeneity, both within and between gold particles, increases the chances of generating a highly unrepresentative signature when small sample sets are employed. A prior characterization of the inclusion suites is highly beneficial to the interpretation of elemental responses generated by quadrupole-MS systems.

While the microchemical characterization of sample populations either by a combination of EPMA and SEM or by quadrupole-LA-ICP-MS is best served by using relatively large sample suites of > 150 particles, we recognize that the ideal may not be attainable for various reasons. In addition, we acknowledge that useful information can still be forthcoming when studies have smaller sample suites at their disposal, particularly when undertaking characterization via other approaches such as crystallography or isotopic analyses where the range of inter-particle variation may be smaller. Nevertheless, interpretation of data sets during gold compositional studies should be informed by the potential for variation in their chemical and physical characteristics which have been presented here.

## Conclusions

Studies of around 40,000 gold particle sections have identified generic microfabrics of alloy heterogeneity, while a combination of compositional and crystallographic analytical approaches on specific particles has illuminated their genesis and constrained the relative timing of their formation. Key outcomes of the study are itemized below:

i. Populations of gold particles formed in the same mineralizing event commonly exhibit alloy heterogeneity both within and between particles. At the micron scale, heterogeneity may be present as mineral inclusion suites, variations in alloy compositions or both.

ii. Additions of Ag-rich alloy to pre-existing gold may take place through equilibration with later fluids. Large-scale replacement independent of grain boundary control is most likely a result of an evolving hydrothermal system, whereas Ag-rich tracks and compositionally complex thin zones spatially sympathetic to grain boundaries may be formed later within the hypogene environment.
iii. Residence in surficial environments can preferentially remove Ag by dissolution along grain boundaries or from the particle margins, while Au remains.
iv. All evidence available to the study favors rim formation by Ag removal rather than Au addition.
v. The Ag ranges of gold from specific styles are greater than previously reported and are not mutually exclusive between gold formed in different deposit styles. Therefore, ascribing a source style to an individual particle on the basis of the Ag content of the Au alloy is intrinsically flawed. Levels of minor alloying elements detectable by EPMA or LA-ICP-MS (Cu, Hg, Pd) may prove valuable discriminants. In general, LA-CP-MS techniques provide a better method to generate quantitative data for these elements than EPMA.
vi. Mineral inclusions are primary features inherited by detrital gold particles and may be the single most important source of data because they represent the mineralogy of an eroded auriferous orebody. Historically, the low incidence of inclusions in some sample populations has discouraged workers from adopting systematic screening in a standard workflow. We strongly advocate the value of inclusions in a wide range of gold-particle studies. The quantification of inclusion abundance in polished sections presented here suggests that 150 particles are required to generate robust data. In addition, the data show that failure to identify inclusions in a small sample set does not indicate their absence.
vii. Images from LA-ICP-(ToF)MS systems have illuminated the pronounced spatial heterogeneity of trace elements in natural gold and have greatly aided interpretation of data from much larger data sets generated using quadrupole-LA-ICP-MS systems. All data sets indicate high levels of trace element heterogeneity, both within and between particles from the same locality, disproving the notion of a uniform distribution of trace elements within gold alloy. Instead, trace elements present either as "clusters"—i.e., localized, but low concentrations within Au alloy or as components of inclusions of other minerals.
viii. The strands of information gained from the various analytical techniques may be synthesized to yield complete physical and chemical characterization of a gold particle. This process is achieved most easily by a systematic application of different techniques, in which reconnaissance is undertaken by BSE imaging in conjunction with an EDS facility. EBSD may be applied to selected targets to identify microstructures and textures that are spatially associated with compositional variations, which may inform on their relationship to the primary ore-forming stage. Subsequent operation of site-specific analysis by EMP, or LA-ICP-MS can be informed by this prior characterization.
ix. The nature and origins of major- and trace-element heterogeneity within gold particles highlight issues for studies which utilize whole-particle analysis or partial sampling of individual particles without prior evaluation of compositional features.
x. Analysis using quadrupole-LA-ICP-MS systems does not permit characterization of sample populations using smaller numbers of particles than currently used for conventional SEM–EPMA studies because of the potential to generate highly unrepresentative results.
xi. Characterization of the microfabrics observed in gold particles through a combination of crystallographic and compositional approaches permits the development of insights into processes of ore formation and could form a useful addition to the tools available for paragenetic study of ore deposits.
xii. New understanding of the nature of trace-element heterogeneity both within gold alloy and associated inclusions provides an insight into the trace-element composition of mineralizing fluids.

**Supplementary Information** The online version contains supplementary material available at https://doi.org/10.1007/s00126-020-01036-x.

**Acknowledgments** The authors would like to acknowledge Dr. Patrick Trimby (Oxford Instruments) for the provision of the EDS/EBSD map (using the Symmetry EBSD detector) shown in Fig. 4C–F. The manuscript benefitted greatly from constructive reviews and comments from Professor Dave Craw, Dr. Norman Moles, Professor Erik Melchiorre, an anonymous reviewer, and Dr. Alexandre Cabral whose input went beyond that of the handling editor. M. Styles publishes with permission of the Executive Director British Geological Survey

## References


Alam M, Li SR, Santosh M, Yuan MW (2018) Morphology and chemistry of placer gold in the Bagrote and Dainter streams, northern Pakistan: implications for provenance and exploration. Geol J 54: 1672–1687

Antweiler JC, Campbell W (1977) Application of gold compositional analyses to mineral exploration in the United States. J Geochem Explor 8:17–29

Argapadmi W, Toth ER, Fehr MA, Schönbächler M, Heinrich CA (2018) Silver isotopes as a source and transport tracer for gold: a reconnaissance study at the Sheba and new consort gold mines in the Barberton Greenstone Belt, Kaapvaal Craton, South Africa. Econ Geol 113:1553–1570

Arif J, Baker T (2004) Gold paragenesis and chemistry at Batu Hijau, Indoneisa: implications for gold-rich porphyry copper deposits. Mineral Deposita 39:523–535

Banks DA, Chapman RJ, Spence-Jones C (2018) Detrital gold as a deposit-specific indicator mineral by LAICP-MS analysis. Geosci BC Rep:2018–2021 http://www.geosciencebc.com/s/2016-006.asp

Bergman H, Piazolo S (2012) The recognition of multiple magmatic events and pre-existing deformation zones in metamorphic rocks as illustrated by CL signatures and numerical modelling: examples from the Ballachulish contact aureole, Scotland. Int J Earth Sci 101: 1127–1148

Beilby G (1921) Aggregation and flow of solids. Macmillan, London

Boyle RW (1979) The geochemistry of gold and its deposits. Geol Surv Can Bull:280p

Brügmann G, Brauns M, Maas R (2019) Silver isotope analysis of gold nuggets: an appraisal of instrumental isotope fractionation effects and potential for high-resolution tracing of placer gold. Chem Geol 516:59–67

Cabral AR, Lehmann B, Kwitco R, Cravo Costa CH (2002a) The Serra Pelada Au-Pd-Pt deposit Carajás Mineral province northern Brazil: reconnaissance mineralogy and chemistry of very high grade palladiferous gold mineralization. Econ Geol 97:1127–1138

Cabral AR, Lehmann B, Kwitko R, Jones RD (2002b) Palladian gold and palladium arsenide–antimonide minerals from Gongo Soco iron ore mine, Quadrilátero Ferrífero, Minas Gerais, Brazil. Appl Earth Sci 111:74–80

Cabral AR, Lehmann B (2007) Seleniferous minerals of palladium and platinum from ouro preto-bearing mineralisation in Brazil. Ore Geol Rev 32:681–688

Cabral AR, Tupinambá M, Lehmann B, Kwitko-Ribeiro R, Vymazalová A (2008a) Arborescent palladiferous gold and empirical $Au_2Pd$ and $Au_3Pd$ in alluvium from southern Serra do Espinhaço, Brazil. Neues Jahrbuch für Mineralogie-Abhandlungen: J Mineral Geochem 184: 329–336

Cabral AR, Suh CE, Kwitko-Ribeiro R, Rocha Filho OG (2008b) Brittle microstructures in gold nuggets: a descriptive study using backscattered electron imaging. Ore Geol Rev 33:212–220

Cabral AR, Ließmann W, Lehmann B (2015) Gold and palladium minerals (including empirical $PdCuBiSe_3$) from the former Roter Bär mine, St. Andreasberg, Harz Mountains, Germany: a result of low-temperature, oxidising fluid overprint. Mineral Petrol 109:649–657

Chapman RJ, Mortensen JK (2006) Application of microchemical characterization of placer gold grains to exploration for epithermal gold mineralization in regions of poor exposure. J Geochem Explor 91:1–26

Chapman RJ, Mortensen JK (2016) Characterization of gold mineralization in the northern Cariboo gold district, British Columbia, Canada, through integration of compositional studies of lode and detrital gold with historical placer production: a tEPMAlate for evaluation of orogenic gold districts. Econ Geol 111:1321–1345. https://doi.org/10.2113/econgeo.111.6.1321

Chapman RJ, Leake R, Moles NR, Earls G, Cooper C, Harrington K, Berzins R (2000a) The application of microchemical analysis of alluvial gold grains to the understanding of complex local and regional gold mineralization: a case study in the Irish and Scottish Caledonides. Econ Geol 95:1753–1773

Chapman RJ, Leake RC, Moles NR (2000b) The use of microchemicalanalysis of alluvial gold grains in mineral exploration: experiences in Britain and Ireland. J Geochem Explor 71: 241–268

Chapman RJ, Leake RC, Floyd J (2000c) Gold mineralization in the vicinity of Glengaber burn, Scottish Borders. Scott J Geol 36:165–176

Chapman RJ, Shaw M, Leake RC, Jackson B (2005) Gold mineralisation in the central Ochil Hills, Perthshire, UK. T I Min Metall B Appl Earth Sci 114:53–64

Chapman RJ, Leake RC, Warner RA, Cahill MC, Moles NR, Shell CA, Taylor JJ (2006) Microchemical characterisation of natural gold and artefact gold as a tool for provenancing prehistoric gold artefacts: a case study in Ireland. Appl Geochem 21:904–918

Chapman RJ, Leake RC, Bond DP, Stedra V, Fairgrieve B (2009) Chemical and mineralogical signatures of gold formed in oxidizing chloride hydrothermal systems and their significance within populations of placer gold grains collected during reconnaissance. Econ Geol 104:563–585

Chapman RJ, Mortensen JK, Crawford EC, Lebarge WP (2010a) Microchemical studies of placer and lode gold in the Klondike District, Yukon, Canada: 1. Evidence for a small, gold-rich, orogenic hydrothermal system in the bonanza and Eldorado Creek area. Econ Geol 105:1369–1392. https://doi.org/10.2113/econgeo.105.8.1369

Chapman RJ, Mortensen JK, Crawford EC, Lebarge WP (2010b) Microchemical studies of placer and lode gold in the Klondike District, Yukon, Canada: 2. Constraints on the nature and location of regional lode sources. Econ Geol 105:1393–1410. https://doi.org/10.2113/econgeo.105.8.1393

Chapman RJ, Mortensen JK, LeBarge WP (2011) Styles of lode gold mineralization contributing to the placers of the Indian River and Black Hills Creek, Yukon Territory, Canada as deduced from microchemical characterization of placer gold grains. Mineral Deposita 46:881–903

Chapman RJ, Allan MM, Grimshaw MR, Mortensen JK, Wrighton TM, Casselman S (2014) Pathfinder signatures in placer gold derived from Au-bearing porphyries. In: MacFarlane KE, Nordling MG, Sack PJ (eds) Yukon Exploration and Geology. Yukon Geological Survey, pp 21–31

Chapman RJ, Mileham TJ, Allan MM, Mortensen JK (2017) A distinctive Pd-Hg signature in detrital gold derived from alkalic Cu-Au porphyry systems. Ore Geol Rev 83:84–102

Chapman RJ, Allan MM, Mortensen JK, Wrighton TM, Grimshaw MR (2018) A new indicator mineral methodology based on a generic Bi-Pb-Te-S mineral inclusion signature in detrital gold from porphyry and low/intermediate sulfidation epithermal environments in Yukon territory, Canada. Mineral Deposita 53:815–834

Chapman T, Clarke GL, Piazolo S, Robbins VA, Trimby PW (2019) Grain-scale dependency of metamorphic reaction on crystal plastic strain. J Metamorph Geol 3:1021–1036

Chugaev AV, Chernyshev IV (2012) High-noble measurement of 107Ag/109Ag in native 435 silver and gold by multicollector inductively coupled plasma mass spectrometry (MC436 ICP-MS). Geochem Int 50:899–910

Craw D, Lilly K (2016) Gold nugget morphology and geochemical environments of nugget formation, southern New Zealand. Ore Geol Rev 79:301–315

Crawford EC (2007) Klondike placer gold: new tools for examining morphology, composition and crystallinity: unpublished M.Sc. thesis, The University of British Columbia, 151 p

Craw D, McLachlan C, Negrini M, Becker N (2017) Quantification and prediction of bulk gold fineness at placer gold mines: a New Zealand example. Minerals 7:226

Desborough GA, Heidel RH, Raymond WH (1971) Primary distribution of silver and copper in native gold from six deposits in the Western United States. Mineral Deposita 6:321–334. https://doi.org/10.1007/BF00201890

Dongmo FWN, Chapman RJ, Bolarinwa AT, Yongue RF, Banks DA, Olajide-Kayode JO (2018) Microchemical characterization of placer gold grains from the Meyos-Essabikoula area, Ntem complex, southern Cameroon. J Afr Earth Sci 1(151):189–201

Dunn SC, Bjorn P, Rozendaal A, Taljaard R (2019) Secondary gold mineralization in the Amani placer gold deposit, Tanzania. Ore Geol Rev 107:87–107

Falconer DM, Craw D, Youngson B, Faure K (2006) Gold and sulfide minrals in tertiary quartz pebble conglomerate gold placers, Southland, New Zealand. Ore Geol Rev 28:525–545

Fisher NH (1945) The fineness of gold, with special reference to the Morobe gold field, New Guinea. Econ Geol 40:449–495

Fuanya C, Bolarinwa AT, Kankeu B, Yongue RF, Ngatcha RB, Tangko TE (2019) Morphological and chemical assessment of alluvial gold grains from Ako'ozam and Njabilobe, southwestern Cameroon. J Afr Earth Sci 154:111–119

Galbiatti HF, Cabral AR, Lehmann B, Kwitko-Ribeiro R (2009) "Ouro preto" found at Timbopeba iron-ore deposit, Minas Gerais, Brazil. Neues Jahrbuch für Geologie und Paläontologie-Abhandlungen 253:15–23

Gammons CH, Williams-Jones AE (1995) Hydrothermal geochemistry of electrum; thermodynamic constraints. Econ Geol 90:420–432. https://doi.org/10.2113/gsecongeo.90.2.420

Gas'kov IV (2017) Major impurity elements in native gold and their association with gold mineralization settings in deposits of Asian folded areas. Russ GeolGeophys 58:1080–1092

Groen JC, Craig JR, Rimstidt JD (1990) Gold–rich rim formation on electrum grains in placers. Can Mineral 28:207–228

Grimshaw MR (2018) Gold mineralisation in the Lone Star area of the Klondike Gold District, Yukon, Canada. PhD thesis, University of Leeds

Halfpenny A, Hough RM, Verrall M (2013) Preparation of samples with both hard and soft phases for electron backscatter diffraction: examples from gold mineralization. Microsc Microanal 19:1007–1018

Hancock EA, Thorne AM (2011) Mineralogy of lode and alluvial gold from the western Capricorn Orogen, Western Australia. Aus J Earth Sci 58:793–801

Henney PJ, Styles MT, Bland DJ, Wetton PD (1994) Characterization of gold from the Lubuk Mandi area, Terengganu, Malaysia: British Geological Survey, Technical Report WC/94/21, 28 p

Henney PJ, Styles MT, Wetton PD, Bland DJ, (1995) Characterization of Gold from the Penjom area near Kuala Lipis, Pahang, Malaysia. British Geological Survey, Technical Report WC/95/21, 23 p

Holness MB, Watt GR (2001) Quartz recrystallization and fluid flow during contact metamorphism: a cathodoluminescence study. Geofluids 1:215–228

Hough RM, Butt CR, Reddy SM, Verrall M (2007) Gold nuggets: supergene or hypogene? Aus J Earth Sci 54:959–964

Hough RM, Butt CR, Fischer-Bühner J (2009) The crystallography, metallography and composition of gold. Elements 5:297–302

Kamenov GD, Melchiorre EB, Ricker FN, DeWitt E (2013) Insights from Pb isotopes for native gold formation during hypogene and supergene processes at Rich Hill, Arizona. Econ Geol 108:1577–1589

Kerr G, Falconer D, Reith F, Craw D (2017) Transport-related mylonitic ductile deformation and shape change of alluvial gold, southern New Zealand. Sediment Geol 361:52–63

Koglin N, Cabral AR, Brunetto WJ, Vymazalová A (2012) Gold–tourmaline assemblage in a Witwatersrand-like gold deposit, Ouro Fino, Quadrilátero Ferrífero of Minas Gerais, Brazil: the composition of gold and metallogenic implications. N.Jb. Miner. Abh: J Mineral Geochem 189:263–273

Knight JB, Mortensen JK, Morison SR (1999a) Lode and placer gold composition in the Klondyke District, Yukon territory, Canada: implications for the nature and genesis of Klondyke placer and lode gold deposits. Econ Geol 94:649–664

Knight JB, Morison SR, Mortensen JK (1999b) The relationship between placer gold particle shape, rimming, and distance of fluvial transport as exEPMAlified by gold from the Klondike District, Yukon territory, Canada. Econ Geol 94(5):635–648

Knight JB, Leitch CH (2001) Phase relations in the system Au–Cu–Ag at low temperatures, based on natural assemblages. Can Mineral 39: 889–905

Krupp RE, Weiser T (1992) On the stability of gold-silver alloys in the weathering environment. Mineral Deposita 27:268–275

Lalomov AV, Chefranov RM, Naumov VA, Naumova OB, LeBarge W, Dilly RA (2016) Typomorphic features of placer gold of Vagran cluster (the northern Urals) and search indicators for primary bedrock gold deposits. Ore Geol Rev 85:321–335. https://doi.org/10.1016/j.oregeorev.2016.06.018

LeFort D, Hanley J, Guillong M (2011) Subepithermal Au-Pd mineralization associated with an alkalic porphyry cu-au deposit, Mount Milligan, Quesnel Terrane, British Columbia, Canada. Econ Geol 106:781–808

Leake RC, Bland DJ, Styles MT (1991) Internal stucture of Au-Pd-Pt grains from south Devon, England, in relation to low-temperature transport and deposition. T I Min Metall B 100:159–178

Leake RC, Bland DJ, Cooper C (1992) Source characterization of alluvial gold from mineral inclusions and internal compositional variation. Trans Inst Mining Metall (Section B Appl Earth Sci) 102:65–82

Leake RC, Chapman RJ, Bland DJ, Condliffe E, Styles MT (1997) Microchemical characterization of gold from Scotland. T I Min Metall B 102:65–82

Leake RC, Chapman RJ, Bland DJ, Stone P, Cameron DG, Styles MT (1998) The origin of alluvial gold in the Leadhills area of Scotland: evidence from internal chemical characteristics. J Explor Geochem 63:7–36

Lind A (1996) Microstructural stability and the kinetics of textural evolution. Dissertation, University of Leeds

Loen JS (1994) Origin of placer gold nuggets and history of formation of glacial gold placers, Gold Creek, Granite County, Montana. Econ Geol 89:91–104

Loen JS (1995) Use of placer gold characteristics to locate bedrock gold mineralization. Explor Min Geol 4:335–339

MacKenzie DJ, Craw D (2005) The mercury and silver contents of gold in quartz vein deposits, Otago Schist, New Zealand. New Zealand J Geology Geophys 48:265–278

McCready AJ, Parnell J, Castro L (2003) Crystalline placer gold from the Rio Neuquen, Argentina; implications for the gold budget in placer gold formation. Econ Geol 98:623–633

McTaggart KC, Knight, JB (1993) Geochemistry of lode and placer gold of the Cariboo District, BC: British Columbia Ministry of Energy, Mines and Petroleum Resources, Open File 30 25 p

Melchiorre EB, Kamenov GD, Sheets-Harris C, Andronikov A, Leatham WB, Yahn J, Lauretta DS (2017) Climate-induced geochemical and morphological evolution of placer gold deposits at Rich Hill, Arizona, USA. GSA Bull 129:193–202

Melchiorre EB, Henderson J (2019) Topographic gradients and lode gold sourcing recorded by placer gold morphology, geochemistry, and mineral inclusions in the east fork San Gabriel River, California, USA. Ore Geol Rev 109:348–357

Minter WEL (1999) Irrefutable detrital origin of Witwatersrand gold and evidence of eolian signatures. Econ Geol 94:665–670

Moles NR, Chapman RJ (2019) Integration of detrital gold microchemistry, heavy mineral distribution and sediment

geochemistry to clarify regional metallogeny in glaciated terrains: application in the Caledonides of southeast Ireland. Econ Geol 114: 207–232

Moles NR, Chapman RJ, Warner R (2013) The significance of copper concentrations in natural gold alloy for reconnaissance exploration and understanding gold-depositing hydrothermal systems. Geochem Expl Environ Anal 13:115–130

Morgan DJ, Jollands MC, Lloyd GE, Banks DA (2014) Using titanium-in-quartz geothermometry and geospeedometry to recover temperatures in the aureole of the Ballachulish Igneous Complex, NW Scotland. Geol Soc Lond, Spec Publ 394:145–165

Morrison GW, Rose WJ, Jaireth S (1991) Geological and geochemical controls on the silver content (fineness) of gold in gold-silver deposits. Ore Geol Rev 6:333–364. https://doi.org/10.1016/0169-1368(91)90009-V

Mountain BW, Wood SA (1988) Chemical controls on the solubility, transport and deposition of platinum and palladium in hydrothermal solutions: a thermodynamic approach. Econ Geol 83:492–510

Naden J, Henney PJ (1995) Characterisation of gold from Fiji. British Geological Survey Technical Report WC/95/41, 31p

Naden, J, Styles, MT, Henney PJ (1994) Characterization of gold from Zimbabwe: Part 1. Bedrock gold: British Geological Survey Technical Report WC/94/51. 1994,100p

Nevolko PA, Kolpakov VV, Nesterenko GG, Fominykh PA (2019) Alluvial placer gold of the Egor'evsk district (northern-Western Salair):composition characteristics, types and mineral microinclusions. Russ Geol Geophys 60:67–85

Oberthür T, Melcher F, Weiser TW (2017) Detrital platinum-group minerals and gold in placers of south-eastern Samar Island, Philippines. Can Mineral 54:45–62

Olivo GM, Gauthier M, Bardoux M (1995) Palladium-bearing gold deposit hosted by Proterozoic Lake superior type Iron formation at the Cauê iron mine, Itabira District, southern Sao Fransisco Craton, Brazil: geologic and structural controls. Econ Geol 90:118–134

Omang BO, Suh CE, Lehmann B, Vishiti A, Chombong NN, Fon AN, Egbe JA, Shemang EM (2015) Microchemical signature of alluvial gold from two contrasting terrains in Cameroon. J Afr Earth Sci 112: 1–4

Outridge PM, Doherty W, Gregoire DC (1998) Determination of trace elemental signatures in placer gold by laser-ablation inductively coupled plasma mass spectrometry as a potential aid for gold exploration. J Geochem Explor 60:229–240

Palacios C, Hérail G, Townley B, Maksaev V, Sepúlveda F, de Parseval P, Rivas P, Lahsen A, Parada MA (2001) The composition of gold in the Cerro Casale gold-rich porphyry deposit, Maricunga belt, northern Chile. Can Mineral 39:907–915

Parnell J, Earls G, Wilkinson JJ, Hutton DHW, Boyce AJ, Fallick AE, Ellam RM, Gleeson SA, Moles NR, Carey PF, Legg I (2000) Regional fluid flow and gold mineralization in the Dalradian of the Sperrin Mountains, Northern Ireland. Econ Geol 95:1389–1416

Pitfield PEJ, Styles MT,Taylor CD, Key, RM, Bauer, W, Ralison A (2010) Gold deposit styles and placer gold characterisation in northern and east-central Madagascar In: 10th Biennial SGA Meeting, Townsville, Australia, 17–20 Aug 2009. 741–743

Piazolo S, Jessell MW, Bons PD, Evans L, Becker JK (2010) Numerical simulations of microstructures using the Elle platform: a modern research and teaching tool. J Geol Soc India 75:110–127

Piazolo S, Austrheim H, Whitehouse M (2012) Brittle-ductile microfabrics in naturally deformed zircon: deformation mechanisms and consequences for U-Pb dating. Am Mineral 97:1544–1563

Piazolo S, La Fontaine A, Trimby P, Harley S, Yang L, Armstrong R, Cairney JM (2016) Deformation-induced trace element redistribution in zircon revealed using atom probe tomography. Nature comm 7:1–7

Potter M, Styles MT (2003) Gold characterization as a guide to bedrock sources for the Estero Hondo alluvial gold mine, western Ecuador. T I Min Metall (Section B Appl Earth Sci) 112:297–304

Prior DJ, Trimby PW, Weber UD, Dingley DJ (1996) Orientation contrast imaging of microstructures in rocks using forescatter detectors in the scanning electron microscope. Min Mag 60:859–869

Prior DJ, Boyle AP, Brenker F, Cheadle MC, Day A, Lopez G, Timms NE (1999) The application of electron backscatter diffraction and orientation contrast imaging in the SEM to textural problems in rocks. Am Mineral 84:1741–1759

Putnis A (2009) Mineral replacement reactions. Rev Mineral Geochem 70:87–124

Reith F, Fairbrother L, Nolze G, Wilhelmi O, Clode PL, Gregg A, Parsons JE, Wakelin SA, Pring A, Hough R, Southam G (2010) Nanoparticle factories: biofilms hold the key to gold dispersion and nugget formation. Geology 38:843–846

Reith F, Stewart L, Wakelin SA (2012) Supergene gold transformation: secondary and nano-particulate gold from southern New Zealand. Chem Geol 320:32–46

Reith F, Rea MA, Sawley P, Zammit CM, Nolze G, Reith T, Rantanen K, Bissett A (2018) Biogeochemical cycling of gold: transforming gold particles from arctic Finland. Chem Geol 483:511–529

Satsukawa T, Piazolo S, González-Jiménez JM, Colás V, Griffin WL, O'Reilly SY, Kerestedjian TN (2015) Fluid-present deformation aids chemical modification of chromite: insights from chromites from Golyamo Kamenyane, SE Bulgaria. Lithos 228:78–89

Sayab M, Suuronen JP, Molnár F, Villanova J, Kallonen A, O'Brien H, Lahtinen R, Lehtonen M (2016) Three-dimensional textural and quantitative analyses of orogenic gold at the nanoscale. Geology 44:739–742

Shuster J, Reith F (2018) Reflecting on gold geomicrobiology research: thoughts and considerations for future endeavors. Minerals. 8:401

Shuster J, Johnston CW, Magarvey NA, Gordon RA, Barron K, Banerjee NR, Southam G (2015) Structural and chemical characterization of placer gold grains: implications for bacterial contributions to grain formation. Geomicrobiol J 32:158–169

Spence-Jones CP, Jenkin GRT, Boyce AJ, Hill NJ, Sangster CJS (2018) Tellurium, magmatic fluids and orogenic gold: an early magmatic fluid pulse at Cononish gold deposit, Scotland. Ore Geol Rev 102: 894–905

Spruzeniece L, Piazolo S, Maynard-Casely HE (2017) Deformation-resembling microstructure created by fluid-mediated dissolution–precipitation reactions. Nat Commun 8:1–9

Standish CD, Dhuime B, Chapman RJ, Hawkesworth CJ, Pike AW (2014) The genesis of gold mineralisation hosted by orogenic belts: a lead isotope investigation of Irish gold deposits. Chem Geol 15: 40–51

Stewart J, Kerr G, Prior D, Halfpenny A, Pearce M, Hough R, Craw D (2017) Low temperature recrystallisation of alluvial gold in paleoplacer deposits. Ore Geol Rev 88:43–56

Styles MT, Wetton, PD, Bland, DJ (1995) Characterization of gold from Zimbabwe part 2: Alluvial and soil Gold. BGS Technical Report WC/95/5

Svetlitskaya TV, Nevolko PA, Kolpakov VV, Tolstykh ND (2018) Native gold from the Inagli Pt–Au placer deposit (the Aldan Shield, Russia): geochemical characteristics and implications for possible bedrock sources. Mineral Deposita 53:323–338

Townley BK, Hérail G, Maksaev V, Palacios C, de Parseval P, Sepulveda F, Orellana R, Rivas P, Ulloa C (2003) Gold grain morphology and composition as an exploration tool: application to gold exploration in covered areas. Geochem Expl Environ Anal 3:29–38

Voisey CR, Maas R, Tomkins AG, Brauns M, Brügmann G (2019) Extreme silver isotope variation in orogenic gold systems implies multistaged metal remobilization during ore genesis. Econ Geol 114:233–242

Von Gehlen K (1983) Silver and mercury in single gold grains from the Witwatersrand and Barberton, South Africa. Mineral Deposita 18: 529–534

Watling RJ, Herbert HK, Delev D, Abell ID (1994) Gold fingerprinting by laser-ablation inductively coupled plasma- mass spectrometry. Spectrochim Acta 49B-2:205–219

Webster JG (1986) The solubility of Au and Ag in the system Au-Ag-S-O2-H2O at 25 °C and 1 atm. Geochim Cosmochim Acta 50:245–255

Webster JG, Mann AW (1984) The influence of climate, geomorphology and primary geology on the supergene migration of Au and Ag. J Geochem Explor 22:21–42

Wrighton TM (2013) Placer gold microchemical characterization and shape analysis applied as an exploration tool in western Yukon. Unpublished MSc thesis, University of British Columbia. 140p

Youngson JH, Craw D (1993) Gold nugget growth during tectonically induced sedimentary recycling, Otago, New Zealand. Sediment Geol 84:71–88

Youngson JH, Craw D (1995) Evolution of placer gold deposits during regional uplift, Central Otago, New Zealand. Econ Geol 90:731–745

Youngson JH, Craw D (1999) Variation in placer style, gold morphology, and gold particle behavior down gravel bed-load rivers; an example from the Shotover/arrow-Kawarau-Clutha River system, Otago, New Zealand. Econ Geol 94:615–633

Youngson JH, Wopereis P, Kerr LC, Craw D (2002) Au-Ag-Hg and Au-Ag alloys in Nokomai and Nevis valley placers, northern Southland and Central Otago, New Zealand, and their implications for placer-source relationships. New Zealand J Geol Geophys 4:53–69

Zaykov VV, Melekestseva IY, Zaykova EV, Kotlyarov VA, Kraynev YD (2017) Gold and platinum group minerals in placers of the south Urals: composition, microinclusions of ore minerals and primary sources. Ore Geol Rev 85:299–320